This is to certify that the

thesis entitled

An Investigation of the Feasibility of Using Sol--Gel Derived Thin Films Toward Development of Optical Sensors

presented by

Dilum Devike Dunuwila

has been accepted towards fulfillment of the requirements for

M.S. degree in Chem. Eng.

Major professor

Date 8/6/93

AN INVESTIGATION OF THE FEASIBILITY OF USING SOL-GEL DERIVED THIN FILMS TOWARD DEVELOPMENT OF OPTICAL SENSORS

By

Dilum Devike Dunuwila

A THESIS

Submitted to
Michigan State University
in partial fulfillment of the requirements
for the degree of

MASTER OF SCIENCE

Department of Chemical Engineering

1993

Abstract

An Investigation Of The Feasibility Of Using Sol-Gel Derived Thin Films Toward Development Of Optical Sensors

By

Dilum Devike Dunuwila

A variety of porous optically transparent titanium alkoxide carboxylate films that can be supported on silicate glass substrates have been developed. These films were made by spin casting intermediate polymeric solutions of alkoxide carboxylates processed using sol-gel techniques. A variety of appropriate probe molecules can be entrapped or immobilized within the porous polymer matrix of these films. These porous films, being optically transparent and having the capability to host probe molecules - probe molecules with characteristic optical properties being more relevant - provided an excellent system to investigate the possibility of making optical sensors. As a model system we picked a colorimetric reagent, Fe(III) porphyrin, as the probe molecule to detect free cyanide ion concentrations in aqueous solutions. Entrapment of the porphyrin was the method of choice. Entrapment was accomplished by direct dissolution of the porphyrin in the sol-gel solutions. Chemically induced structural modifications of the polymer were carried out to stabilize the encapsulated metalloporphyrin. A detailed account of the synthesis of this model sensing system and its response are presented. An optical parameter reflective of the chemical changes that occur in the system was selected as the measurement tool and its calibration was linear over the cyanide ion concentration range of 40 ppm to 25,000 ppm.

I dedicate this work to my dear parents, in gratitude for their selfless sacrifices made over the years to provide an opportunity for me and my sister for fulfillment in our lives.

Acknowledgments

I would like to thank my advisor Dr. Kris Berglund for providing me with an opportunity to experience the excitement of discovery.

Table of Contents

List of Tables

List of Figures

1 Overview

Hydrolysis of alkoxides of a variety of metals, often under mild conditions, leads to polymeric solutions or gels. The pathway that leads to such polymeric species is recognized as the sol-gel process. The sol-gel process has received much attention in industry and in academia since it affords the capability to synthesize a wide range of new materials with unique properties. Mild process conditions make the process a more economically viable one. The versatility of sol-gel processed materials, essentially porous sol-gel glasses, rests on their high level of homogeneity. The high internal surface area and the favorable optical properties provide for a wide range of applications including system analysis using optical absorption, fluorescence and Raman scattering.

Under controlled conditions, solution precursors of sol-gel systems can be prevented from congealing into gels. Stable solutions thus obtained can be used to make thin films supported on various substrates using dipping, spin casting and deposition techniques. These thin films, although processed differently, retain the structural integrity characteristic of porous sol-gel glasses along with high internal surface area and favorable optical properties.

The primary objective of this research was to investigate the possibility of making an optical sensing system for small chemical species such as free cyanide ions in aqueous solutions using sol-gel related thin films. In order to reach this objective it was necessary to make a thin film that can be employed as a host to colorimetric reagents chemically sensitive

to a given chemical species that can diffuse through the pore structure of the film. The sensing system is conceptualized in Figure 1.1.

As mentioned before, controlled hydrolysis in sol-gel systems is the key to making thin films. Probably the most promising technique available for the control of hydrolysis of highly reactive alkoxides is to use chelating organic ligands such as glycols, organic acids and β-diketones. These chelating ligand effectively occupy some of the coordination sites of the alkoxide lowering the rate and extent of hydrolysis. The related chemistry is discussed extensively in the following chapter. A series of thin films that were porous, optically transparent, mechanically stable and resistant to aqueous and organic solvents were developed by controlled hydrolysis of titanium(IV)isopropoxide using carboxylic acids of varying chain length as the chelating ligands. Spin casting was used exclusively to process the films.

The metal center of metalloporphyrins have a very high affinity to electron donor ligands such as cyanide ions. In addition, metalloporphyrins, in general porphyrins, have characteristic absorption maxima in their UV-visible absorption spectra. Among these bands, the Soret band which occurs around the UV-visible transition region, in general, has the highest absorptivity. The quartet of bands that appear in the visible region is related to the symmetry of the macro cyclic molecule. When donor ligands such as cyanide ions react with metalloporphyrins the resulting electron redistribution alters the fine structure of the molecule causing the Soret band to shift to the red with respect to its original position, i.e. the energy of the π–π^* transition is effectively lowered. The relative absorptivity of the two absorption maxima depends on the metalloporphyrin and cyanide concentrations, i.e., it depends on the

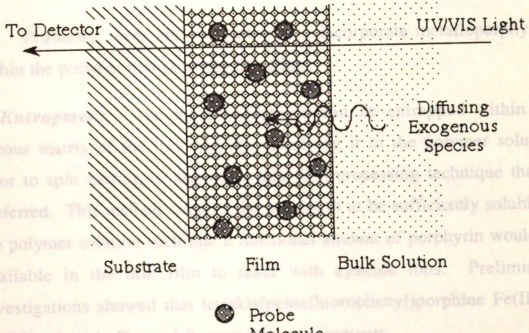

Figure 1.1 Configuration of the sensor system.

the reactants. Therefore, at constant porphyrin concentration, the relative absorptivities can be calibrated with the initial cyanide concentrations. It should also be noted that cyanide ions, placed at the high end of the electrochemical series, have a particularly high affinity toward metalloporphyrins. The cyanide and metalloporphyrin system, having favorable chemical and spectroscopic phenomenon discussed above, was selected for this investigation.

Primarily, there are two methods to incorporate metalloporphyrins within the polymer matrix of the thin films.

a) ***Entrapment:*** The metalloporphyrin can be entrapped within the porous matrix of the thin film by dissolving it in the polymer solution prior to spin casting or any other thin film processing technique that is preferred. This method requires the porphyrin to be sufficiently soluble in the polymer solution such that a functional amount of porphyrin would be available in the thin film to react with cyanide ions. Preliminary investigations showed that tetrakis(pentafluorophenyl)porphine Fe(III)Cl (PFPP), given in Figure 1.2, meets the requirements.

b) ***Covalent immobilization:*** Metalloporphyrins can be covalently linked to the polymer matrix of the thin films through chelating ligands such as organic acid groups that are attached to the peripheral ring of the porphyrin. However, steric effects of the bulky porphyrin macro cyclic molecule may substantially hinder such substitution reactions.

The investigation focused mostly on entrapment since techniques for the conformation of immobilization through covalent linkage were not

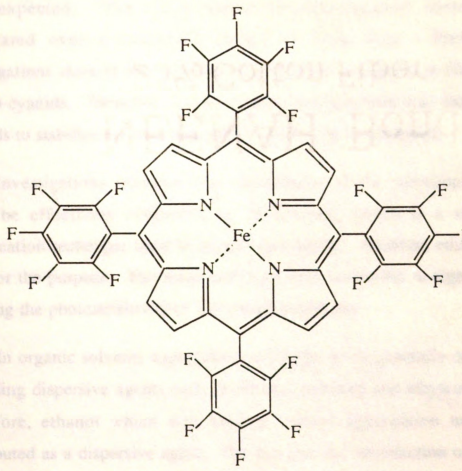

Figure 1.2 Molecular structure of tetrakis(pentafluorophenyl)porphine-Fe(III)Cl, (PFPP).

developed at the time.

Porphyrins are known to aggregate into dimers and sometimes into stacked oligomers in solution. They are also photosensitive. Such instabilities of the metalloporphyrin, especially in the entrapment mode, were expected. The encapsulated metalloporphyrin continuously aggregated over a monitored period of fifty days. Preliminary investigations showed that aggregated porphyrins entrapped in films were inert to cyanide. Therefore, a more stable sensing system was desired and methods to stabilize the metalloporphyrin had to be investigated.

Investigations revealed that aggregation of the metalloporphyrin could be effectively controlled by alcoholysis, which is a structural modification technique used in sol-gel processing. Absolute ethanol was used for the purpose. The same technique was successful in significantly reducing the photosensitivity of the metalloporphyrin.

In organic solvents aggregation of porphyrins is generally controlled by adding dispersive agents such as ethanol, pyridine and ethylene glycol. Therefore, ethanol which was used to control aggregation may have contributed as a dispersive agent. The fact that the introduction of ethanol stabilized aggregation is conclusive; however, the exact mechanism is not obvious.

Following the development of a stable sensing system, the relative absorbance of the cyano-metalloporphyrin and the metalloporphyrin was calibrated against the natural logarithm of the free cyanide ion concentration. The calibration was linear from 40 ppm to 25,000 ppm cyanide ion concentration. Even though the lower limit of this model sensing system is not sufficiently low for most analytical purposes, the

applicability of alkoxide carboxylate films in such devises is clearly demonstrated.

Most chemical sensing systems are based on wet-chemistry techniques. These techniques require elaborate laboratory equipment, trained personnel and a considerable amount of time to analyze samples. In contrast dry-chemistry techniques such as the one investigated here where all necessary reagents are contained in dry form in a strip allows an untrained person to measure the concentration of a substance using a standard calibration. These devises can be used to analyze streams of pharmaceutical processes, agricultural and industrial waste effecting the environment and can also be used in human and animal diagnosis.

In addition to the simplicity and the operational ease common to dry-chemistry techniques, the sol-gel method used to make the structure of the sensor in this model system makes such systems very cost effective. Ambient conditions and small amounts of precursors are used. Mass production of these sensor strips can be easily accomplished and packaging poses no difficulty. Inexpensive hand held spectrophotometers are available for quick analysis when needed.

2 Literature Review

2.1 The Sol-Gel Process

2.1.1 Background

In 1846 Ebelmen [1] observed the gradual transformation of a clear silicone alkoxide solution, open to atmospheric humidity, into a transparent solid; a gel in relevant terminology. It was also observed that the metallo-organic gel thus formed produces a silicon dioxide network upon heating. However, it was not until the late 1960s that the observations now studied in detail as the sol-gel process received attention both from an academic and industrial standpoint. Search for new ceramic materials for application in electronics, solar energy conversions, optics, catalysis, membrane technologies etc., sparked a considerable growth of the field of sol-gel processing. The sol-gel process, in particular, was of interest due to the versatility of the process by which one could make tailored material of high purity and homogeneity. Also, the process was practically and economically feasible due to low temperature process conditions, direct molding capabilities and need for only simple processing facilities. Good mechanical, chemical and thermal stability and high porosity are characteristic of these materials. In addition optically transparent material can be processed without much difficulty.

Sol-gel processed thin films have also received much attention over the years. Methods used for preparation include spin casting, dip coating and sputter depositing of sol-gel solutions on suitable supports.

Structurally the film are not much different from gels and they acquire the same characteristics seen in gels

Films prepared by sol-gel techniques have applications in many areas. They are used as protective coatings against corrosion of metals. They are also used to stabilize chemically less durable glasses and against humidity effects on electronic equipment. Certain properties of substrates can be modified using these coatings; adjustment of hardness of materials and adjustment of reflectivity or refractivity of material. Thin film optical filters can be made utilizing absorption phenomena of alkoxide transition metals. Material for heat insulation, electrical conductors and surface acoustic wave guides (SAW) are among other specific applications. Porous thin films can also be used as the structural basis of responsive chemical sensors where spectroscopic methods are applied as analytical devises.

2.1.2 The Sol-Gel Chemistry

The sol-gel process comprises a set of reversible chemical reactions that occur when water is introduced to a metal alkoxide. A simplified reaction scheme is given below.

(I) *Hydrolysis:*

$$M(OR)_4 + nH_2O \rightleftharpoons M(OR)_{4-n}(OH)_n + nROH \qquad (2.1)$$

(II) *Condensation:*

$$2\,M(OR)_{4-n}(OH)_n \rightleftharpoons M(OR)_{4-n}(OH)_{n-1}\text{—}O\text{—}M(OR)_{4-n}(OH)_{n-1} + H_2O \qquad (2.2)$$

$$2\,M(OR)_{4-n}(OH)_n \rightleftharpoons M(OR)_{3-n}(OH)_n\text{—}O\text{—}M(OR)_{4-n}(OH)_{n-1} + ROH \qquad (2.3)$$

(III) *Aggregation:*

$$M(OR)_{4-n}(OH)_n + M(OR)_4 \rightleftharpoons M(OR)_{4-n}(OH)_{n-1}(OH)\cdots\rightarrow M(OR)_4 \qquad (2.4)$$

$$2M(OR)_4 \rightleftharpoons M(OR)_3{-}(OR)\cdots\rightarrow M(OR)_4 \qquad (2.5)$$

Where M denotes the metal and R denotes the alkyl group

(I) ***Hydrolysis:*** When water is introduced to a tetravalent metal alkoxide, an alkoxy group, (−OR), of the alkoxide is replaced by the nucleophilic attack of the oxygen atom of a hydroxyl ion. Generally, the reaction is fast; however, it can be limited by the metal shielding effect of bulky alkyl groups. If desired, acid or base catalysis can be used to drive the reaction to rapid completion [2]. Solvents like alcohols, acetone or dioxane, that introduce homogeneity to the reaction mixture, can promote hydrolysis [2]. These solvents help by dissolving hydrolyzed species that are otherwise insoluble.

(II) ***Condensation:*** Condensation also occurs via nucleophilic attack by oxygen atoms. However, the groups involved are somewhat different. Here, the oxygen atom of a metal hydroxy group displaces a hydroxyl or alkoxy group of a second tetravalent metal (reactions (2) and (3)) generating water or the corresponding alcohol. It should be noted that water generated in reaction (2) is available for further hydrolysis of potential sites. It is the condensation reaction that leads monomeric tetravalent alkoxides to oligomers and finally to polymers unified by metal-oxygen networks. Even though, the simple reaction scheme presented does not indicate such network formation, the possibility is evident.

(III) ***Aggregation:*** Aggregation occurs via nucleophilic addition, distinct from nucleophilic substitution which is the mechanism for

hydrolysis and condensation. The oxygen atom of a hydroxyl group or a alkoxy group attached to the metal, having a lone pair of electrons, undergoes a nucleophilic addition reaction (reactions (4) and (5)) to a second tetravalent metal. This type of reaction occurs when the coordination sphere of a metal is not saturated. It follows that this phenomenon is prevalent when going from main-group metals to transition metals and lanthanides [3]. Other related reactions, olation (nucleophilic substitution of aquo groups of hydrated metal alkoxides by metal hydroxy groups) and oxolation (formation of oxo bridges, M−O−M, through nucleophilic addition) have been studied [3]. The latter reaction, being an addition reaction, occur when the metal coordination is not completely saturated. Regardless of the type of reaction aggregation promotes polymeric network formation.

The three types of reactions described above occur at different rates and to different extents depending on process conditions. The reactions collectively drive the system toward a polymeric configurations that constitutes a gel with different degrees of hydrolysis, condensation and aggregation. This process that begins with a molecular solution which then undergoes several stage transitions through chemical reactions - dimers to oligomers to polymeric networks - is called the sol-gel process.

2.1.3 Sol-Gel Solutions: Hydroxide Precipitation

Most metal alkoxides hydrolyze upon contact with water precipitating metal hydroxides. With relevance to sol-gel processed gels, films and fibers, such precipitation leads to inhomogeneity in the final structure. Therefore, preparation of homogeneous solutions by controlling precipitation is essential to process high quality products. Precipitation can be facilitated by two mechanisms [4]. They are, precipitation by chemical

reactions that produce insoluble species and precipitation by physical agglomeration where precipitation occurs when dissolved particles nucleate and grow upon reaching saturation. Precipitation by chemical reaction is easily controlled by modifying precursors and mechanisms. However, physical agglomeration is harder to control since phase equilibria at various experimental conditions for these systems are less apparent.

(I) ***Physical Precipitation:*** Solid alkoxides can precipitate from alkoxide solutions in crystalline or amorphous form and growth leading to agglomeration can ensue. Changing parameters such as temperature and solvent can increase the nucleation energy barrier and the supersaturation limit, facilitating some degree of control of solubility. Solution pH is another parameter that can be adjusted to control physical precipitation.[4]. However, the direct synthesis of the alkoxide is said to be the most practical method for the control of physical precipitation; the effective solubility of an alkoxide in a solvent used in the direct synthesis method can be several orders of magnitude higher compared to the dissociation solubility of the alkoxide in the same solvent [4].

(II) ***Chemical Precipitation:*** Chemical precipitation in sol-gel solutions occur when reactions of alkoxides with water or any other nucleophilic reagent produce insoluble products. The solubility and therefore the precipitation of these products are governed by the same parameters that were presented under physical precipitation; thus, control parameters discussed under physical precipitation applies. However, due to the nature of the mechanism leading to chemical precipitation, additional control strategies that are more easily handled are available. They are change of water or reagent concentration, modification of precursors and mode of water addition [4].

As discussed before, the sol-gel chemistry involves hydrolysis of alkoxides and subsequent polycondensation of resulting hydroxides. The rate of hydrolysis, r_h, and the rate of polycondensation, r_p, are affected differently by temperature changes. Therefore, changes in temperature can cause wide variations in the ratio (r_h/r_p). Given that pure hydroxide tend to form precipitates and the polycondensates tend to form homogeneous solutions, a decrease in the ratio (r_h/r_p) by temperature adjustment would lead to favorable homogeneous solutions. A barium isopropoxide system studied by Zheng et al. [4] suggests that high temperatures causes a lowering of the ratio (r_h/r_p) which in turn leads to clearer gels. However, the universal applicability of this phenomenon is not clear since in systems where acid or base catalysis is employed the rates are markedly modified by pH.

Addition of nucleophilic reagents to alkoxides and substitution of alkoxy groups of alkoxides by nucleophilic reagents can reduce the degree of hydrolysis and also the rate of hydrolysis. The degree of hydrolysis is reduced as a result of these reagents occupying the coordination sites of the alkoxides. The hydrolysis rate reduction occurs due to modifying nucleophilic reagents having higher resistance to substitution by hydroxy groups. Consequently, hydrolysis and therefore precipitation are better controlled. Such nucleophilic reagents include alcohols, silanols, organic esters, silyl esters, glycols, organic acids, anhydrides and alkanolamines. Depending on the hygroscopicity, coordination number and reactivity of the alkoxide the amount of control exerted on a particular system may vary.

The amount of water and the mode of introduction of water greatly influence the reactions leading to precipitation or gelation of sol-gel

solutions. It is expected that higher water concentrations would promote hydrolysis and therefore precipitation. Related effects were studied by Prassas [5] and Lacourse [6]. In certain systems it has been observed that absorption of atmospheric water by alkoxide solutions leads to homogeneous solutions while dropwise or bulk addition of water leads to instant precipitation [7]. The reaction of alkoxides with absorbed water is homogeneous and gradual compared to the dropwise or bulk introduction of water where an instantaneous heterogeneous reaction takes place. The kinetics of the two different mechanisms are such that the product homogeneity is affected. Another method for water introduction that is reported to work is introducing the amount of water required through water loaded silica gel [8].

2.1.4 Chemical Modification of Sol-Gel Processing

The chemistry of metal alkoxides is such that it facilitates many avenues for synthesizing tailor-made materials. The stages of the sol-gel process - monomeric, oligomeric and polymeric - can be controlled and altered chemically to obtain desired materials. Chemical interactions of the alkoxides and modifying reagents that facilitate modification through control and alteration are as follows [9]:

- relative changes in ionic character of the metal-oxygen bond due to electronegativity differences between the metal and the oxygen atom;
- inductive effects of the alkyl group of the alkoxide can induce significant changes to the polarity of the metal-oxygen bond altering the susceptibility of the bond to nucleophilic attack;

- the tendency of metal alkoxides to form stable or meta stable oligomers by saturating its coordination sphere by means of dative intermolecular bonds with donor atoms of adjacent alkoxide molecules.

It is evident from the above considerations that the selection of the metal and the alkyl group of the alkoxide and the introduction of appropriate modifying nucleophilic reagents or solvents can lead to new materials with chemically modified structures. How the selection of precursors and addition of reagents lead to structural modifications at the distinct stages of the sol-gel process will be discussed in the context of the chemical considerations presented above.

(I) ***Oligomerization in Alkoxide Solutions:*** Molecular association of alkoxide molecules in solution is an important consideration as it can influence the morphology and physical properties of final products. Molecular association occurs as a result of the tendency of metals to saturate their coordination spheres. Alkoxide molecules consisting of electron donor groups bind to adjacent alkoxide molecules through dative intermolecular bonds. This coordination sphere expansion process occurs as a result of vacant metal orbitals accepting oxygen lone pairs from alkoxy ligands. These agglomerates hydrolyze and polycondense at different rates and to different extents compared to their monomeric counterparts due to their thermodynamic stability. This results in significant structural and physical changes in final products.

The degree of oligomerization depends on the nature of the metal and also on the alkoxy groups that constitute the metal alkoxide. In some instances it has been shown that the solvent and solute concentration has an effect on the degree of oligomerization. The effect of both the metal atom

and the alkoxy group on the degree of oligomerization is shown in Tables 2.1 and 2.2 respectively .

In general larger metals tend to achieve a higher coordination number. This implies that the degree of oligomerization increases with the size of the metal. Conversely, the degree of oligomerization decreases with greater length, increased branching and increased bulkiness of alkoxy groups. These trends are clearly evident in the data presented in Tables 2.1 and 2.2.

Oligomerization that is dependent on solvent and solute concentration has been observed with titanium alkoxide derivatives. Lower association has been correlated to lower solute concentrations [10]. Bradley et al. [11] observed that ethanol breaks down oligomers while benzene does not. This phenomenon has been attributed to ethanol having the capability to complete the coordination sphere of the metal of dissociated oligomeric species.

(II) ***Hydrolysis:*** Hydrolysis is the reaction that initiates the sol-gel process. Regardless of the molecular nature of the metal alkoxide - monomeric or oligomeric - hydrolysis initiates the process. However, rates at which reactions take place and the extents to which reactions proceed may vary significantly depending on the molecular nature of the metal alkoxide precursor. This in turn will determine the relative changes that can be expected in the processed materials.

Once hydrolysis occur and metal hydroxides are formed condensation takes place leading to polymeric species. Once initiated, hydrolysis and polycondensation generally take place simultaneously and the final form of the polycondensates very much depend on the rate and the

Table 2.1 [9] Degree of oligomerization as a function of metal size.

Compound	$Ti(OEt)_4$	$Zr(OEt)_4$	$Hf(OEt)_4$	$Th(OEt)_4$
Covalent Radii(A^o)	1.32	1.45	1.44	1.55
Degree of Oligomer	2.4	3.6	3.6	6.0

Et=ethyl

Table 2.2 [9] Degree of oligomerization as a function of length and branching of the alkoxy group.

	Et	Bu^n	Bu^s	Bu^t	$CH_3(CH_2)_4$	$(C_2H_5)_2CH$	$(CH_3)_2(C_2H_5)C$
$Ti(OR)_4$	2.4	3	-	1.0	1.4	1.0	1.0
$Zr(OR)_4$	3.6	3.4	-	1.0	-	2.0	1.0
$Al(OR)_4$	4.1	3.9	2.4	1.95	4.0	2.08	1.97

OR=alkoxy group, Et=etyl, Bu=butyl, n=normal, s=secondary, t=tertiary

extent of hydrolysis. Since the nature of the polycondensates, in most part, is a consequence of hydrolysis, polycondensation will not be discussed separately.

Most metal alkoxides are highly reactive with water and the reactions produce insoluble precipitates. As was discussed in section 2.1.3-(II) the ratio (r_h/r_p) should be controlled, generally lowered, to obtain homogeneous polymeric solutions. To some extent the rate of hydrolysis and the degree of hydrolysis can be reduces by using under stoichiometric quantities of water. However, more effective and more manageable techniques are available and they will be discussed shortly.

Hydrolysis of metal alkoxides and subsequent product forms have received much attention in the literature. Many product forms and formulations for systems under varying conditions have been proposed [11, 12]. Titanium alkoxides, according to most of these studies, react very fast with water followed by slower rates of polycondensation. Lowering the rate of hydrolysis as mentioned earlier is of primary importance to the synthesis of homogeneous material. The attempt at controlling the rate and extent of hydrolysis in many studies has been successful. The rate of hydrolysis of titanium alkoxides, in general, is lower when the alkyl chain length of the alkoxy group is longer and also when the group configuration is secondary or tertiary [13]. This trend is attributed to the bulkiness of longer chains and non primary structures that inhibit hydrolysis through steric effects. Kamia et al. [14] have also presented a controlled hydrolysis method used to obtain preferential molecular structure for the preparation of TiO_2 fibers.

Utilization of more stable or controllable metal alkoxide precursors is probably the most effective method for controlling the rate and extent of

hydrolysis. Metal alkoxides of different elements and different alkoxy groups exhibit a wide range of reactivities with water leading to structurally and physically diverse materials.

Reactivities can be controlled by sequential hydrolysis where appropriate reagent are added following tested sequences [15] or by reactivity matching techniques where appropriate reagents are utilized [16].

Precursor stability can also be achieved by reacting metal alkoxides with chelating organic ligands such as glycols, organic acids or β-diketones. The stability of metal alkoxides chelated by such ligands is attributed to the fact that multidentate chelation is inherently more stable than monodentate binding. Thermodynamic data that conforms the stabilizing chelate effects are available and the predictability of desired products from chemical reactions of chelated complexes has been proven [17]. The extent of stability that a particular chelating ligand gives is determined by the nature of the donor atoms, the ring size and the nature of the coordination sphere around the central metal.

Glycols show high molecular association with metal alkoxides according to the reaction

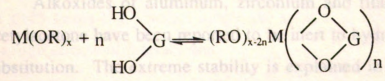

$$M(OR)_x + n \begin{matrix} HO \\ \diagdown \\ G \\ \diagup \\ HO \end{matrix} \rightleftharpoons (RO)_{x-2n}M\left(\begin{matrix} O \\ \diagup \quad \diagdown \\ G \\ \diagdown \quad \diagup \\ O \end{matrix}\right)_n + 2n\,ROH \qquad (2.6)$$

where G=alkyl or alkylene group, M=metal and R=alkyl group. Resulting chelates exhibit more resistance to hydrolysis than the parent metal alkoxide [13]. Guizard et al. [18] were successful in controlling hydroxide precipitation of zirconium alkoxides by reacting ethylene glycol with the

alkoxide. The controlled hydrolysis sequence resulted in transparent monolithic gels.

Metal alkoxides are known to react with organic acids according to the reaction

$$M(OR)_n + x\ R'COOH \rightleftharpoons M(OR)_{n-x}(OOCR')_x + x\ ROH \qquad (2.7)$$

where, R' is any alkyl group. Further, monodentate or bidentate chelation of the acid ligand to the metal is possible. For example, molecular forms as illustrated below may result.

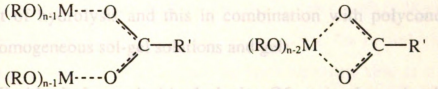

Monodentate Chelation Bidentate Chelation

Both Doeuff et al. [19, 20] and Sanchez et al. [21] used acetic acid to control hydroxide precipitation of $Ti(OBu^n)_4$ successfully. These authors showed that acetate complexed as bidentate ligands are not easily substituted by hydroxide, unlike the facile substitution of alkoxy groups by hydroxides.

Alkoxides of aluminum, zirconium and titanium complexing with acetylacetone have been reported to be inert to hydrolysis and in general to substitution. The extreme stability is explained in terms of the electronic charge distribution over the six membered ring that forms when acetylacetone is chelated with the metal [22]. The six membered ring formation is illustrated below.

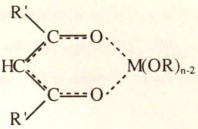

Chelation does not prevent the hydrolysis of remaining alkoxy groups and subsequent polycondensation. It only lowers the rate of hydrolysis and the extent of hydrolysis by occupying the coordination sites of the metal either temporarily (glycols and organic acids) or permanently (β-diketones). In general the technique lowers the rate of hydrolysis and the extent of hydrolysis and this in combination with polycondensation leads to homogeneous sol-gel solutions and gels.

(III) ***Alcohols and Alcoholysis:*** Often in the sol-gel process alcohols are used as the solvent. However, unlike most other solvents that are chemically inert, alcohols partake in the scheme of reactions that takes place in the sol-gel process. Two cases can be considered:

(1) the metal alkoxide dissolved in its parent alcohol,

(2) the metal alkoxide dissolved in an alcohol other than its parent alcohol.

In both cases the alcohol alters the nature of metal alkoxide precursors through chemical interactions.

As discussed previously metals tend to saturate their coordination sites by expansion. Alcohols having lone pairs can promote expansion of the coordination sphere by donating the lone pairs to the metal through dative bonds. An increase in the gelation time of a $Si(OMe)_4$–$B(OMe)_3$ sol-gel system due to the above mentioned interaction was reported by Woignier et al. [23].

Alcohol is a product of the hydrolysis reaction given in Equation 2.1. Therefore, introduction of the parent alcohol to the system externally influences the equilibrium. As a result a lower extent of hydrolysis can be expected.

When alcohols other than the parent alcohol is used the primary chemical interaction is alcohol interchange or in alternate terminology, alcoholysis. The reaction can be represented simply as:

$$M(OR)_n + x\ R'OH \rightleftharpoons M(OR)_{n-x}(OR')_x + x\ ROH \qquad (2.8)$$

In systems where a combination of metal alkoxides with different alkoxy groups are used, alcohols can be utilized to match the hydrolysis rates of the alkoxides [9]. With relevance to such systems, this is a versatile technique for the control of hydrolysis of alkoxides possessing very different reactivities, as is often the case.

Alcoholysis proceeds via an S_N2 mechanism and therefore it is significantly influenced by steric effects. Bulky alkoxy groups are more easily substituted by less bulky alkoxy groups. This trend for titanium alkoxides was verified by Verma et al. [24]. The same trend, due also to steric effects, is sometimes promoted by higher degrees of oligomerization of the metal alkoxide precursors [9].

In an open system, where volatile alcohols can be distilled out, alcohol interchange can be driven if the replaced alcohol is more volatile than the substituted alcohol. The same objective can be accomplished by performing alcoholysis with alcohols that produce insoluble alkoxides. In this instance the phase separation drives the reaction to completion. This type of phase separation is observed when methanol is added to titanium ethoxide or titanium isopropoxide [24].

Following the above discussion it is fair to say that alcohols, in addition to being good solvents for sol-gel systems, are very effective in controlling hydrolysis and final structural properties of sol-gel derived materials. Therefore, the sensible selection of alcohols can lead to tailor-made sol-gel material.

2.1.5 Sol-Gel Processed Thin Films

The sol-gel process comprises of identifiable dynamic stages. Once hydrolysis of the alkoxide precursor is initiated the molecular precursors are transformed to oligomers and then to polymers that eventually congeal into homogeneous gels. However, controlled hydrolysis techniques (see section 2.1.4) allows the preparation of stable intermediate polymeric solutions that do not proceed to gel formation. These solutions - suitable viscous properties provided - can be used to make coatings, generally in thin film form, using coating techniques such as dipping, deposition or spin casting [25, 26]. Sufficient control of compositions and conditions can lead to thin films of desired properties; homogeneous films without cracking or flaking, porous, optically transparent, good adhesion with chemical - thermal - mechanical stability, solvent resistant and structural distributions favoring stability of incorporated reagents.

Films prepared by sol-gel techniques have applications in many areas. They are used as protective coatings against corrosion of metals. They are also used to stabilize chemically less durable glasses and against humidity effects on electronic equipment. Certain properties of substrates can be modified using these coatings; adjustment of hardness of materials and adjustment of reflectivity or refractivity of material. Thin film optical filters can be made utilizing absorption phenomena of alkoxide transition metals. Material for heat insulation, electrical conductors and surface

acoustic wave guides (SAW) are among other specific applications. Porous thin films can be used as the structural basis of responsive chemical sensors where spectroscopic methods are applied as analytical devises.

Adhesion of the polymeric coating solution to the substrate is an important consideration in making thin films. Adhesion can be reduces by shear stresses at the boundary layer due to mismatch of thermal expansion coefficients, relative differences in moduli of elasticity and mechanical overloads (bending) [25].

All film making techniques involve evaporation of solvent, excess precursors and byproducts resulting in a volume reduction of the film. In pure inorganic systems relaxation along with the volume reduction is difficult due to prevalent excessive cross linking. The brittleness of these materials leads to high shear stresses and as a consequence the material generally demonstrate poor adhesion properties. Sol-gel processing can be effectively used to reduce cross linking and allow easier relaxation properties. The introduction of organic groups to the inorganic matrix of sol-gel material can increase the elasticity of the material. This in turn can improve the ability of film formation of sol-gel polymeric solutions.

As demonstrated in section (2.1.4-(II)), lengthy organic groups can be attached to alkoxide precursors. These groups occupy coordination sites of the metal reducing the amount of inorganic cross linking. Therefore relaxation along with the volume reduction is easily accomplished. The organic groups having sufficient mobility also follow the shrinkage. Monodentate chelating ligands can act as flexible links between inorganic units. The process is illustrated in Figure 2.1. With relevance to sol-gel processed thin films supported on silicate glasses, adhesion is strengthened by Si–O–M coupling where M is the metal of the alkoxide precursor used.

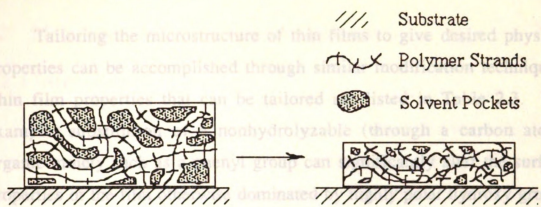

Figure 2.1 [25] Shrinkage of a solvent containing polymer film.

Schmidt et al. [25], working with aluminum alkoxides, showed two cases where organic ligands were used to improve the film formation ability of sol-gel solutions. Aluminum alkoxides modified by both glycerol and acetylacetone led to crack free coatings. TEM (transmission electron microscopy) analysis showed that increased homogeneity of the microstructure relates to better film quality. Schmidt et al. [25] concluded that organic processing (modification of alkoxides by organic ligands) in combination with high homogeneity leads to a good film formation behavior. The following reaction shows how complex formation by organic ligands blocks potential sites for hydrolysis and condensation thus leading to flexible microstructures that demonstrate good film formation behavior.

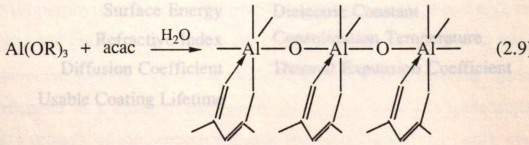

(2.9)

where, acac=acetylacetone.

Tailoring the microstructure of thin films to give desired physical properties can be accomplished through similar modification techniques. Thin film properties that can be tailored are listed in Table 2.3. For example, substitution of a nonhydrolyzable (through a carbon atom) organic moiety such as a phenyl group can significantly alter the surface properties of the film otherwise dominated by highly polar hydroxy groups [26]. A decrease in the total surface energy and in particular the density of polar hydroxy groups can among other things improve the film adhesion qualities to low energy surfaces such as organic polymers. Substituted organic groups can also dramatically decrease the refractive index of thin films. Thomson et al. [27] found that film thickness can be controlled by varying solution and equipment parameters.

Stable coating solutions are of considerable importance in film processing. Stability can be achieved by control techniques where hydrolysis/condensation sites are blocked by nonhydrolyzable moieties or by chelating ligands that are more resistant to hydrolysis compared to alkoxy groups. In general such modifications prevent gelation or increases gelation time allowing a higher usable life time of the coating solutions.

Table 2.3 Tailored sol-gel film properties.

Hardness	Resistivity
Crystallinity	Durability
Surface Energy	Dielectric Constant
Refractive Index	Consolidation Temperature
Diffusion Coefficient	Thermal Expansion Coefficient
Usable Coating Lifetime	

2.2 Metalloporphyrins: A Concise Overview

2.2.1 Structure

The parent ring system given in Figure 2.2 is called a porphyrin [28]. It is often abbreviated as $H_2(P)$, and the abbreviation signifies the acidic sites. The letter P describes the ring system. A porphyrin in which at least one of the acidic sites is substituted by a metal atom is called a metalloporphyrin. Metalloporphyrins are abbreviated by M(P) where the letter M denotes the particular metal. Numerous examples for porphyrins and metalloporphyrins are presented in [29]. In general, the reaction between a porphyrin free acid, $H_2(P)$, and a metal salt, MX_2, produces a metalloporphyrin. The reaction is identified as "metallation" of a $H_2(P)$ and it can be illustrated as in Figure 2.3.

As it is the case with most metals, the four coordinate configuration given in Figure 2.3 does not saturate the available coordination sites of the metal. Therefore, metals tend to acquire additional donor ligands to expand their coordination sphere to a more stable configuration. The donor ligands, Z, coordinate to the metal along the four fold rotational axis of the metalloporphyrin; thus, the ligand are referred to as axial ligands. Axial coordination of donor ligands is illustrated in Figure 2.4.

In transition metals that constitute most of the stable metalloporphyrins, the five 3d orbitals (d_{xy}, d_{xz}, d_{yz}, d_{x2-y2} and d_{z2}), the 4s orbital and the three 4p orbitals (p_x,p_y and p_z) actively partake in bonding to potential ligands. Since the nitrogen atoms of the porphyrin ligand are configured in a square-planar geometry (Figure 2.3) it is quite apparent that s orbitals of the porphyrin ligand and axial ligands can only overlap

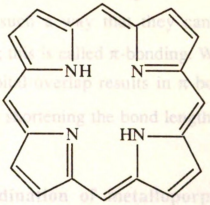

Figure 2.2 Molecular structure of the parent porphyrin

$$H_2(P) + MX_2 \rightleftharpoons M(P) + 2\,HX$$

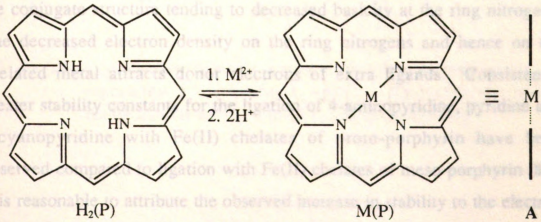

Figure 2.3 Formation of a monometallic metalloporphyrin. A is the bar graph for M(P), showing the projection of the porphyrin plane on to a plane normal to the paper.

with 4s, 4p, $3d_{x2-y2}$ and $3d_{z2}$ orbitals of the metal to form σ coordinated bonds that constitute square-planar, square-pyramidal and octahedral molecular geometries. However, the t_{2g} orbitals (d_{xy}, d_{xz} and d_{yz}) of the metal are oriented in such a way that they can overlap with empty p orbitals of ligand atoms; this is called π-bonding. With ligands such as =N-, CO, O_2 and CN^-, π-orbital overlap results in π-bonds. The phenomenon fortifies the σ-bonds by shortening the bond length; thus, the lability of the complex is reduced.

2.2.2 Further Coordination of metalloporphyrins

Decreased basicity at the nitrogen atoms of metalloporphyrins can offer increased affinity for the donor electrons of axial ligands. The basicity of the porphyrin nucleus is decreased when electron attracting groups are attached at the periphery of the macrocycle. In which case, the electron cloud of the macrocycle is polarized toward the periphery through the conjugate structure tending to decreased basicity at the ring nitrogens. The decreased electron density on the ring nitrogens and hence on the chelated metal attracts donor electrons of extra ligands. Consistently greater stability constants for the ligation of 4-aminopyridine, pyridine and 4-cyanopyridine with Fe(II) chelates of proto-porphyrin have been observed compared to ligation with Fe(II) chelates of meso-porphyrin [30]. It is reasonable to attribute the observed increase in stability to the electron withdrawing effect of vinyl groups present on the proto-porphyrin complex.

High donor capacity of potential axial ligands is not necessarily correlated to high affinity of such ligands to porphyrin metal chelates. Basic ligands are the best electron donors. Conversely, they are the poorest electron acceptors. Therefore, ligated basic ligands resist π-orbital overlap

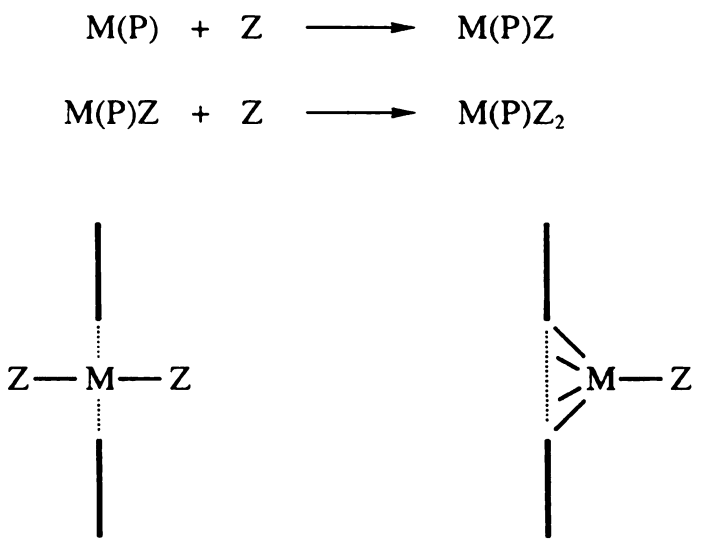

Figure 2.4 Coordination types of a general metalloporphyrin where Z represents a monodentate ligand. Note that the axial configurations are not limited to that given herein.

between the metal t_{2g} orbitals and empty π-orbitals of the ligand, thus limiting the σ-bond reinforcement phenomenon discussed before. The overall result is a relatively weak axial linkage. On the other hand, less basic ligands provide for π-orbital overlap, reinforcing the σ-bond and the overall stability of the complex. For example, 4-aminopyridine which possesses 10^7 times stronger electron donor power than that of 4-cyanopyridine, has a much lower affinity toward ligation to meso-, deutero- and proto-hemes [30].

The extent of back bonding is also affected by the nature of the porphyrin. The results of a study of the reactivities of cyanide with several ferric porphyrins - namely, deutero-, proto- and meso-hemin - showed a significantly high stability for the deutero complex compared to the other hemin complexes [31]. The free base form of the deutero porphyrin is a stronger donor than the proto but a weaker donor than the meso. This results in a compromise between σ- and π-bonding tendencies leading to metal-ligand bond fortification. The order of stability as shown by the results was deutero > proto > meso.

The presence of electrophilic substituents at the periphery of the porphyrin can cause a significant deficiency in π-electron density at the metal center with the consequent outcome of weakened π-bonding between the metal and the axial ligands. This effect is clearly seen when the affinity of 4-cyanopyridine to meso-, deutero-, proto- and diacetyldeutero-heme is compared [30]. The affinity increases from meso- to deutero-heme and then recedes as the electrophilic effects of proto- and diacetyldeutero-heme decreases the π-bonding phenomenon.

Studies with heme proteins have shown evidence for extensive π-orbital overlap between the porphyrin ring and favorably oriented

aromatic moieties of amino acids [32]. The possibility of modifying the reactivities of axial ligand binding utilizing this phenomenon has been investigated [33]. Thermodynamic evidence for such inter-actions between the electron donor molecule 1, 10- phenanthroline and the low-spin complex bis-(imidazole)deuteroporphyrin(IX)dimethylesterFe(III)chloride at a site remote from the metal atom was reported. The presence of 1, 10-phenanthroline in the reaction mixture of imidazole and porphyrin promoted the formation of the bisimidazole complex and in addition stabilized the complex over the reactant. The fact that 1, 10-phenanthroline did not induce any spectral changes in the process suggests that the locus of interaction between the electron donor and the metalloporphyrin is remote from the metal atom. A clear explanation for the structure of the interacting species or the nature of interaction is not available; however, the potential for modification of reactivities of axial ligation and also of the stability of complexes toward improved practical applications is clear.

Hydrogen bonding effects between potential ligands and added solutes can be beneficial in modifying reactivities of ligand binding reactions [34]. Stanford et al. [34] observed a marked increase in the rate of CO binding to Fe(TPP)(imidazole)$_2$ (TPP=tetraphenylporphyrin) when relatively high concentrations of 1, 10-phenanthroline was added to the iron porphyrin and imidazole system. This most likely reflects a hydrogen bonding equilibrium between imidazole and 1, 10-phenanthroline that effectively reduces the concentration of free imidazole available for complexation in the reaction mixture.

Ligands such as cyanide [35, 36], piperidine [36, 37], n-hexanethiol [36] and phosphine [36] induce reduction of ferric porphyrins. The reaction between cyanide and Fe(III)porphyrin produces the low-spin bis-

(cyano)ferric porphyrin. It was observed that this complex then undergoes autoreduction to form ferrous bis-cyanide [35a]. Kinetic data analysis revealed that the observed rate of reduction was linearly dependent on the cyanide concentration. Even though , the cyanide ion is not known for its reducing capacity, the linear dependence of the rate of reduction on the cyanide ion concentration suggests that it is mechanistically involved in the process. A mechanism consistent with the observed linear dependency has been proposed. Nucleophilic attack on the coordinated ferric atom by free cyanide ions present in the reaction medium may homolytically cleave a bond between the metal and a coordinated cyanide ligand, thus, producing a free electron in the vicinity of the metal. This electron in turn may reduce the Fe(III)porphyrin complex to a Fe(II) valency state. In these systems however, the introduction of molecular oxygen reverses the process to yield the initial Fe(III) complex [36, 38]. If indeed the reduction proceeds through this mechanism, more basic porphyrins are expected to be less susceptible to autoreduction since higher electron density placed on the metal atom would resist nucleophilic attack. Evidence conforming this trend was observed by Kadish et al [39]. References for more detailed studies are given in [38].

Solvent effects are important in complexation of metalloporphyrin systems. Proposed solute-solvent interactions affecting complexation reactivities and complex stability's include, the formation of π-complexes and charge transfer complexes, hydrophobic interactions, dipole orientation forces and dispersion forces and hydrogen bonding. Interactions or forces in effect in a particular system may vary from solvent to solvent [40].

2.2.3 Spectra

Many spectroscopic techniques provide insight to physicochemical properties of porphyrins and metalloporphyrins. Among them are, ultraviolet (UV) and visible (VIS) absorption spectroscopy, fluorescence spectroscopy, infrared spectroscopy, nuclear magnetic resonance spectroscopy (NMR) and electron spin resonance spectroscopy (ESR). However, in addition to being very sensitive, UV/VIS absorption spectroscopy is the most convenient technique. It is also very well suited for great practical usefulness due to simple instrumentation and experimental procedures compared to that of other spectroscopic techniques cited above. Only UV/VIS absorption spectroscopy as applied to porphyrin is discussed here. Reviews of other spectroscopic techniques are given in [41, 29].

UV/VIS absorption spectroscopy: A typical absorption spectrum of a porphyrin is given in Figure 2.5. As illustrated in Figure 2.5 the absorption spectra of porphyrin free acids and metalloporphyrins typically include a set of bands in the visible region and an intense absorption band around 400 nm (near UV) [29, 41]. The band that occurs around 400 nm is called the Soret band and the high absorption intensity is very characteristic of the Soret band. The molar extinction coefficient, ε, of the Soret band is in the range 2 to 5×10^5, generally, and the intensity can be 10 to 20 times than that of the strongest visible band [41].

In the case of neutral porphyrins the set of absorption bands in the visible region is made of four distinct bands numbered I-IV. In porphyrin ring systems where peripheral substitution is symmetric the intensity of these bands is in the order IV > III > II > I (Figure 2.5). However, when

asymmetry is introduced to the ring system through peripheral substitution by unlike electron-donor groups or unlike strong electron-withdrawing groups other patterns in intensity distribution is observed. This is attributed to the development of asymmetry in the π-electron cloud of the porphyrin equatorial plane resulting from electron-donating and electron-withdrawing effects of relevant peripheral substituents. The wave length of absorption of all bands, including the Soret band, shifts to longer wave lengths when electron-donor groups are involved and the opposite is true when electron-withdrawing groups are involved.

The set of four bands in the visible region of a neutral porphyrin collapses to a set of two bands upon protonation to a dication, deprotonation to a dianion or metallation by a divalent metal. It is believed that these forms closely resemble a square symmetric configuration [41]. Metallation by metals with higher valency also gives a set of two visible bands; however, the bands shift further to longer wave lengths due to such metals acquiring additional donor ligands at axial positions. It follows that a typical absorption spectrum of a metalloporphyrin consists of a Soret band and two visible bands called α and β bands. However, some metalloporphyrins may exhibit charge-transfer bands. Charge transfer bands, being d-d type transitions, are normally obscured by the other transition bands. The Soret band is the result of electronic transitions of the porphyrin nucleus and it is affected by side-chains, chelation and axial ligands. The α and β bands, on the other hand, arise from the electronic transitions of the metalloporphyrin complex configured with a distinct spatial geometry. Wide variations in wavelengths of absorption, intensities and relative intensity of the α and β bands can be observed when numerous metals are compared.

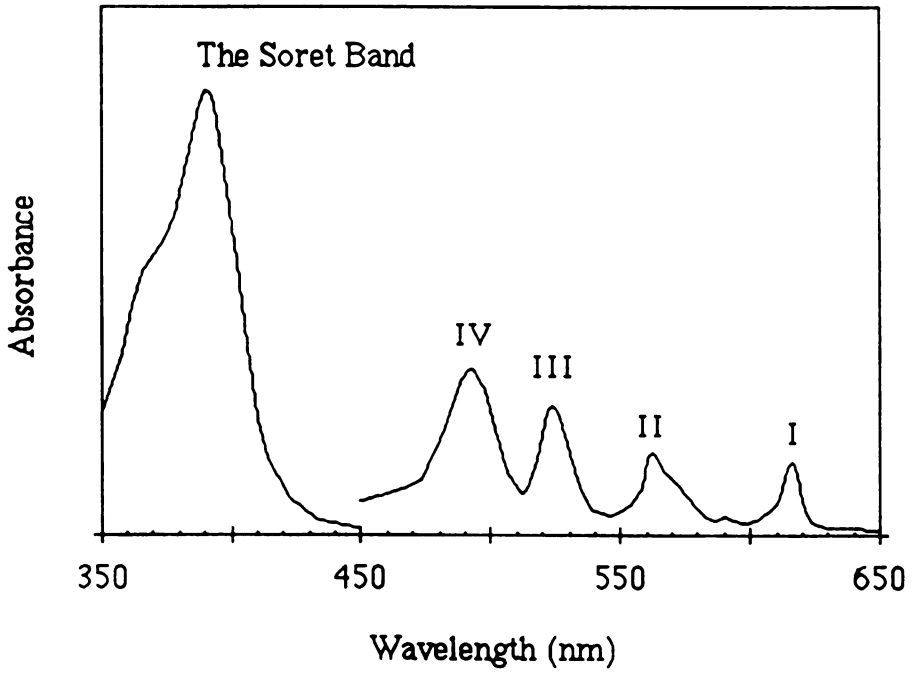

Figure 2.5 Absorption spectrum of octaethylporphyrin (OEP) in acetone. The region 350 - 450 nm (Soret band) is plotted on an absorption scale that is 25 % of the scale for the region 450 - 650 nm.

Iron-porphyrins readily acquire additional ligand at axial positions to form octahedral complexes. Among these ligands are molecules such as water, pyridine, carbon monoxide, or ions such as halides, hydroxide and cyanide [41]. Based on spectral features, metalloporphyrin spectra fall into apparent categories and they can be correlated to the atom through which the ligands are coordinated to the porphyrin complex [41]. It should be noted that while the identification of trends discussed above are more relevant to this work, more extensive classification schemes are available in the literature [29].

2.2.4 Stability of Metalloporphyrins

Metalloporphyrin chelates (square-planar metalloporphyrins with divalent metal ions) and metalloporphyrin complexes (square-pyramidal and octahedral metalloporphyrin compounds formed on addition of extra ligands) demonstrate a high degree of thermodynamic stability. This is due in part to the quadruple binding sites on the porphyrin ligand through which the chelate is formed. The overriding causes for the unusually high thermodynamic stability found in porphyrin metal chelates and complexes are factors associated with the aromaticity of the porphyrin nucleus. More stable porphyrin metal chelates are formed as a result of the metal becoming an integral part of the highly resonant aromatic system. A prime example for the degree of conjugation found in these systems is the influence that electron withdrawing groups on the periphery of the macrocycle have on the further coordination of ligands to the metal [30]. In section 2.2.1 it was mentioned that π-orbital overlap between t_{2g} metal orbitals and empty π-orbitals of axial ligand can lead to conjugation. The complex stability observed in metalloporphyrins made of axial ligands possessing a high affinity for ligation is reflective of this bond

strengthening phenomenon. A case illustration for the relative affinities of ligand to axial ligation appears as, cyanide > imidazole >> pyridine [42].

(I) ***Instability due to Light:*** Some metalloporphyrins are inherently unstable. The causatives for instability and the mechanisms leading to destabilization are numerous. Contact with air and exposure to light is likely to cause photooxidation followed by fission of the metalloporphyrin macrocycle; thus, complexes are more easily demetallated. Light sensitivity of metalloporphyrins is said to be profound with that showing high fluorescence activity and higher stability toward acids [29]. Instability of metalloporphyrins in acid solutions is more common than in organic solutions and are more likely to be stable in benzene than in ether or acetone [29].

Photooxidation [43] and photoreduction [44] of metalloporphyrins have been studied. Protoporphyrin, in benzene or pyridine solutions, gives an oxidation product on exposure to light and molecular oxygen [43]. The zinc complex of α,β,γ,δ-tetraphenyl-porphine is photoreduced to form chlorins* and tetrahydroporphins* in the presence of benzoin [44b].

The effects of X-, β-, γ-irradiation on metalloporphyrins have been studied [45]. All chelates and complexes are not necessarily susceptible to irradiation by all types of radiation. The effects, if at all, depend on the metalloporphyrin and the experimental conditions.

(II) ***Instability in Acid Solutions:*** Concentrated sulfuric acid is often used to dislodge coordinated metals from the porphyrin nucleus. The method takes advantage of the stability of the porphyrin nucleus itself in concentrated sulfuric acid. However, other acids such as perchloric,

* Macrocycles closely related to porphyrins [37].

chromic, permanganate and hydriodic acid disintegrate the porphyrin nucleus as well.

The stability of metalloporphyrins in acid solutions has been classified in terms of a stability index [29]. The stability index takes into account the ratio charge to effective ionic radius and the Pauling electronegativity of the central metal. The electrostatic contribution to the bond energy increases with the ratio charge to effective ionic radius and the Pauling electronegativity enhances the covalent bonding tendency. Thus, a higher charge, a lower ionic radius and high electronegativity of the metal leads to more stable chelates and complexes. For example, porphyrins incorporated with the metals Sn(IV) and Sb(V) that have high charge, high electronegativity and low ionic radii are extremely stable in concentrated acid solutions. On the contrary, metalloporphyrins made of alkali metals and the heavier alkaline earth metals are very labile since these metals posses a low charge, a low electronegativity and a large ionic radius. Other factors such as back bonding from the metal to the porphyrin ligand can also contribute to the stability of metalloporphyrins.

(III) ***Dimerization and Aggregation:*** Dimerization and aggregation of free base porphyrins and metalloporphyrins is frequently encountered in aqueous media. It is an aspect of instability that has received much attention. Many observed property changes have been ascribed to aggregation.

Early work in the area [46, 47] established that porphyrins and their metal derivatives aggregate in a face to face stacked configuration. More recent work [48] has verified the general notion of this model. Most researchers treat aggregation using the dimer model;

$$2\,PH_2 \overset{K_d}{\rightleftharpoons} P_2H_2 \qquad (2.10)$$

The adoption of this model is in most part influenced by its mathematical simplicity; however, further aggregation into units of multiple stacked rings is not ruled out. Many methods such as UV/VIS absorption spectroscopy, potentiometry, electron-spin resonance and temperature jump technique have been used to deduce the nature of stacked units [48].

The presence of aggregate species is easily ascertained through Beer's Law experiments. Deviations from the law observed in the study of porphyrins are consistently cited as evidence for aggregation; however, additional experimental proof is required to verify simple dimerization. Both Cu and Ni complexes of TCPP (tetracarboxyphenylporphyrin) demonstrate Beer's Law deviations in electrolyte solutions [49]. A plot of (absorbance/cell path length) vs. concentration for CuTCPP is given in Figure 2.6 and the non linearity suggests the occurrence of aggregation.

Dilution test plots can be beneficial in discerning simple dimers. The theoretical basis of the dilution test and its application to verify the nature of ferrimesoporphyrin is given by Cowgill et al. [42b]. The splitting of dimeric heme units by both pyridine and imidazole was tested by Gallagher et al. [50] employing dilution test plots.

In the absence of conflicting evidence, the presence of an isosbestic point in dilution studies manifests a monomer-dimer equilibrium. White et al. [51] observed an isosbestic point in the dilution of hexanediamine porphyrin, where the (path length) x (the total porphyrin concentration) is maintained constant. The resulting spectral changes are illustrated in Figure 2.7. The peak at lower wavelength is the dimer absorption peak and upon dilution the absorption maximum red shifts, indicating the splitting of

the dimer to the monomer. The peak at higher wave length is the monomer absorption peak. Shelnutt et al. [50] studied the effect of dilution on Cu coproporphyrin I and a similar pattern was observed. It was established that at concentrations above 5 x 10^{-7} M the blue shifted Soret maximum of the dimer was prevalent, while upon dilution, the peak corresponding to the monomer was increasingly dominant. Dilution of both CuTCPP and NiTCPP give isosbestic points, one in each case, along with the same spectral dynamics observed above [49].

Some porphyrins form π-cation dimers through spin pairing. The formation of dimers results in the complete disappearance of the electron-spin resonance spectrum; hence, a powerful technique when applicable.

The high frequency Raman spectrum of metalloporphyrins contains a number of characteristic lines that are sensitive to the electronic and molecular structure of the porphyrin [50]. Upon dimerization, which is accompanied by changes to the π-electron cloud and the overall structure, the character of these lines is altered and therefore dimerization can be monitored.

Kinetic studies conducted using the temperature jump technique have been helpful in discriminating simple dimerization from aggregation [52]. A theoretical overview is given [48]. Pasternack et al. [49], using temperature jump relaxation experiments, concluded that none of the tetra(N-methylpyridyl)-porphine (TMPyP) complexes of Ni, Cu and Zn aggregated appreciably in solution. Limitations of the technique in determining the distinction between simple dimers and more extensive aggregation have been noted [48].

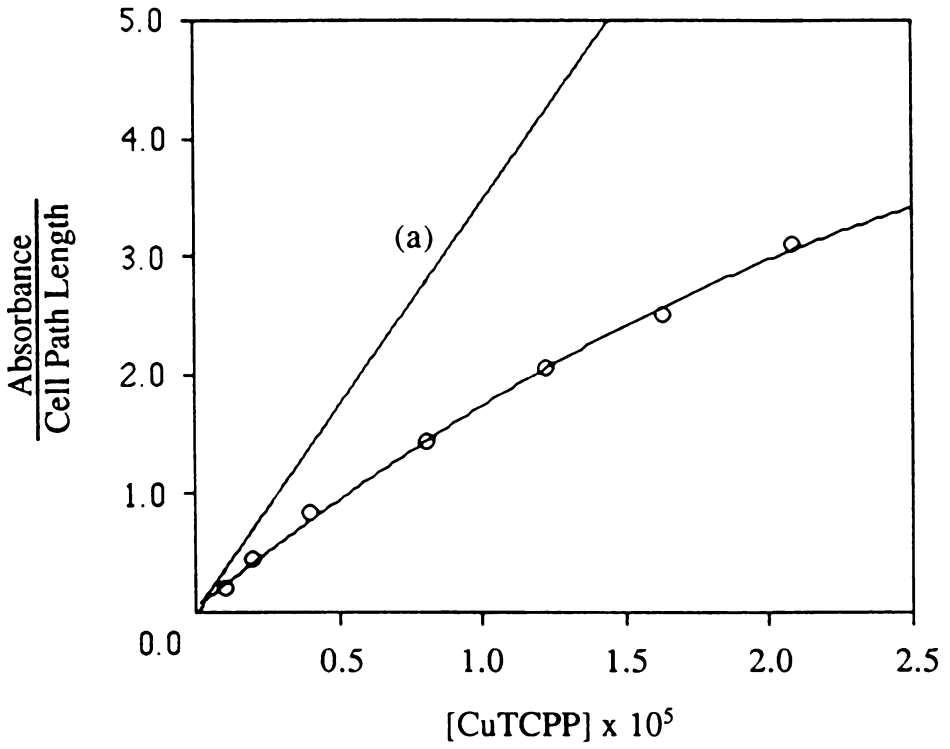

Figure 2.6 [58] Beer's law experiment for CuTCPP (TCPP=tetra-carboxyphenylporphyrin) in aqueous solution. The line marked (a) defines Beer's law behavior for CuTCPP. The curve follows experimental data.

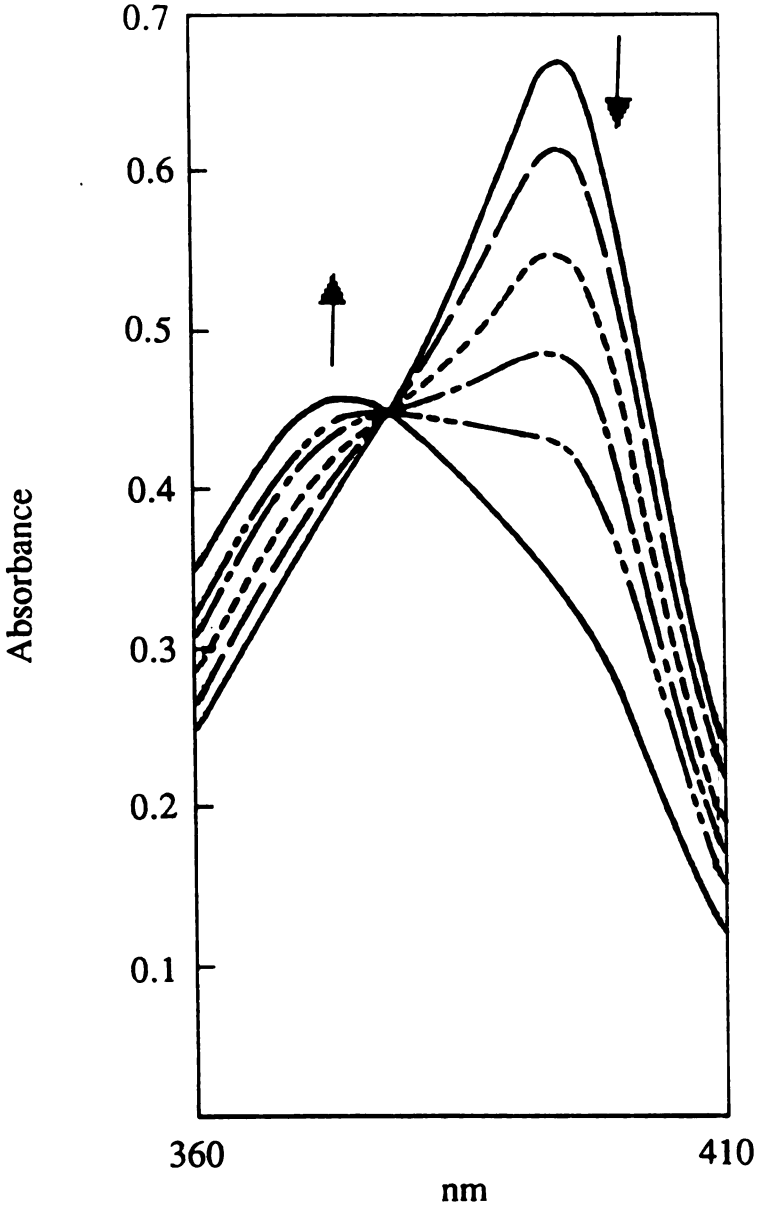

Figure 2.7 [51] Spectral dynamics of hexanediamineporphyrin in the Soret region as a function of hexanediamineporphyrin concentration. The growth of the blue shifted aggregate peak and the disappearance of the monomer peak at high porphyrin concentrations are indicated. In this experiment the product of porphyrin concentration and the cell path length has been maintained a constant.

The extent of aggregation is greatly affected by solvent medium effects. Many solvent additives are known to disperse aggregated species. White et al. [51] reported that the addition of ethanol or ethylene glycol to diamine protoporphyrin IX dimethylesters disperses dimeric units. The dispersion was monitored by following the red shift of the Soret band where the molar absorptivity of the absorption at longer wave length is magnified relative to that at shorter wave length. Kassner et al. [53] obtained monomeric hematoporphyrin and coproporphyrin in a solution comprised of 10% pyridine in water. An occasion where splitting of dimeric ferrimesoporphyrin by pilocarpate and histidine occurred was published by Cowgill et al. [42b]. Both pilocarpate and histidine are derivatives of imidazole. In experiments conducted by Gallagher et al. [54], the titration of dimeric heme with pyridine or imidazole resulted in corresponding monomeric hemochromogens. However, they also observed that the hemochromogens so produced aggregated upon standing. The aggregation was accompanied by a red shift in Soret absorption maximum and a marked decrease in the Soret absorptivity. The latter feature corroborates with results obtained by others; however, in all other cases reviewed here, aggregation was signified by a blue shift in the Soret absorption. If the hemochromogen formation was carried out in an aqueous-alcohol medium the aggregation can be impeded [55]. It is believed that dispersion of aggregates upon the addition of dispersive agents such as those introduced above is predominantly due to the lowering of the dielectric constant of the solvent. The volume percent of dispersive agent in solution is said to be immaterial [48].

The ionic strength of porphyrin solvent media exerts a strong effect on monomeric porphyrin molecules to aggregate. Dimerization and further aggregation are impeded by the like charges on porphyrin

molecules that force molecular dispersion. The addition of an electrolyte provides a large concentration of counterions that screen the principle dispersive forces that prevent porphyrin molecules from aggregating. Thus, in such an environment where the like charges on porphyrin molecules have been effectively neutralized, aggregation usually prevails.

White et al. [51] studied the dimerization constant (K_d) as a function of ionic strength for a series of diamine protoporphyrins. The dimerization constant increased profoundly with added ionic strength. The dimerization constant of numerous porphyrins in various solvent systems and their corresponding references are given [48].

It is expected that porphyrins with peripheral substituents of longer chain length would be screened more readily from each other since the Debye ionic atmosphere of the porphyrin molecules is of the same order of magnitude as the length of the carbon chains [56]. White et al.[51], in their study, pointed out that the dimerization constant of porphyrins with longer chain diamines, at least in some cases, were more significantly effected by added ionic strength than were shorter chain diamine porphyrins. This confirms, to a certain degree, the influence of peripheral substituent's chain length on aggregation.

The influence of charge type at the periphery of the porphyrin molecule on tendencies to aggregate has received some attention in the literature [49, 52a]. It is supposed that positive charges at the periphery of the macrocycle tend to diffuse the charge distribution over the molecule while negative charges at the periphery tend to concentrate the electron density distribution at the center of the molecule. In the case of free base porphyrins the localized electron density distribution at the center enhances van der Waals interactions that promote ring-stacked dimers. However, in

a study of TCPP, which has carboxylate anionic charges at the periphery, Pasternack et al. [49] found little evidence for aggregation of TCPP or its metal derivatives in the absence of added electrolyte. Shelnutt et al. [50] observed that the metallocoproporphyrins are aggregated at much lower concentrations than the corresponding uroporphyrins. Noting that coproporphyrin has uroporphyrin's acetic acid groups substituted by methyl groups, the logical explanation is that the excessive coulombic repulsion resulting from the charge localization on uroporphyrin - due to the acetate ions - impedes the close approach of molecules and thereby prevents aggregation.

An increase in temperature is expected to shift the monomer-dimer equilibrium in favor of the monomer. This was confirmed by a study of the thermodynamics of dimerization for a series of diamine porphyrins by White et al. [51].

2.2.5 Kinetics and Thermodynamics: Methods and Contributing Factors With Emphasis to the Cyanide Ligand

Studies of kinetics and thermodynamics of substitution reactions of metalloporphyrins are abundant in relevant literature. Simple mathematical models that can be used to extract thermodynamic equilibrium constants and reaction rate constants for reactions in solution are available [57, 58, 59,60, 61].

Anation reactions are accompanied by spectral changes that reflect the character of the altered electronic environment imposed by the incoming ligand. Kinetic and thermodynamic parameters for anation reactions can be obtained following these changes. The changes in the Soret region are more practical due to the extent of relative changes that

are normally observed in this region and also due to the high Soret absorbance intensity. Generally observed spectral highlights are, the gradual depletion of the absorption maximum corresponding to unsubstituted metalloporphyrin, the consequent growth of the absorption maximum corresponding to the substituted complex and the isosbestic point that separates the two maxima. Measurement of the changes in absorption intensity at either maximum can be used in simple mathematical models to calculate kinetic and thermodynamic quantities. Somewhat less rigorous, yet informative, mathematical models that have been developed and extensively applied are presented below.

Let MP denote the metalloporphyrin before complexation or substitution, let MPL_n be the complex and let L be the substituting or complexing ligand; then,

$$MP + n\,L \rightleftharpoons MPL_n \qquad (2.11)$$

The thermodynamic equilibrium of Reaction 2.11 can be written as;

$$\log K_n = -n \log[L] - \log\left\{\frac{[MP]}{[MPL_n]}\right\} \qquad [2.1]$$

metalloporphyrin concentrations and the optical absorbance of the system are related by [58];

$$\frac{(A_\infty - A)}{(A - A_o)} = \frac{[MP]}{[MPL_n]} \qquad [2.2]$$

substitution of [2.2] in [2.1] gives;

$$\log\left\{\frac{(A_\infty - A)}{(A - A_o)}\right\} = \log K_n + n \log[L] \qquad [2.3]$$

where, A, A_o and A_∞ denote the absorbance when both absorbing species are present, absorbance prior to complexation or substitution and absorbance at complete complexation or substitution respectively. K_n is the equilibrium constant. A plot of $\log\{(A_\infty - A)/(A - A_o)\}$ vs. log[L] yields a straight line which has a slope equal to the degree of complexation, n, and an intercept described by the equilibrium constant. If A_∞ is not readily available, Equation 2.3 may be rearranged as [58, 62];

$$A = A_\infty - \frac{1}{K_n}\frac{(A - A_o)}{[L]^n} \qquad [2.4]$$

in which case, a plot of A vs. $(A - A_o)/[L]^n$ yields $-(1/K_n)$ as the slope and A_∞ as the intercept. In this case a series of experiments are conducted where a given amount of metalloporphyrin is reacted with varying ligand concentrations; the absorbance measurement is taken at an appropriate wavelength (usually at a wave length where maximum absorption occurs) once the reaction reaches equilibrium. A typical plot is given in Figure 2.8. Improvements in data analysis using alternate methods have been claimed [63].

The kinetic rate expression for Reaction 2.11 can be written as;

$$-\frac{d}{dt}[MP] = (k_1[L] + k_{-1})[MP] - k_{-1}[MP]_o \qquad [2.5]$$

noting that, $[MP]_o = [MP] + [MPL_n]$. $[MP]_o$ is the initial metalloporphyrin concentration. k_1 and k_{-1} are the forward and reverse rate constants respectively and $(k_1[L] + k_{-1}) = k_{obs}$ = (constant), for ligand concentrations in excess. Equation 2.5 can be reduced to;

$$-\frac{d}{dt}\left\{\frac{[MP]}{[MP]_o}\right\} = k_{obs}\left\{\frac{[MP]}{[MP]_o}\right\} - k_{-1} \qquad [2.6]$$

and upon integration gives the following equation.

$$\frac{[MP]}{[MP]_o} = \frac{k_{-1}}{k_{obs}} + \left\{\frac{(k_{obs} - k_{-1})}{k_{obs}}\right\}\exp\{-k_{obs}t\} \qquad [2.7]$$

For ligand concentrations in excess, $k_{obs} >> k_{-1}$; thus,

$$\log\left\{\frac{[MP]}{[MP]_o}\right\} = -k_{obs}t \qquad [2.8]$$

Using $[MP]_o = [MP] + [MPL_n]$ in Equation 2.2 yields;

$$\frac{[MP]}{[MP]_o} = \frac{(A_\infty - A)}{(A_\infty - A_o)} \qquad [2.9]$$

Combining Equations 2.8 and 2.9 gives;

$$\log\left\{\frac{(A_\infty - A)}{(A_\infty - A_o)}\right\} = -k_{obs}t \qquad [2.10]$$

The pseudo first order rate constant, k_{obs}, can be obtained from a plot of $\log\{(A_\infty - A)/(A_\infty - A_o)\}$ vs. t at fixed ligand concentrations. Then, a plot of k_{obs} vs. [L] can be used obtain values for k_1 and k_{-1}. Note that $k_{obs} = (k_1[L] + k_{-1})$. Thus, kinetic data for reactions in solution can be procured in a manner that is quite straight forward. Data acquisition for this calculation requires the time course of each individual experiment of the case discussed earlier to be followed; i.e., absorbance measurements must be acquired at regular time intervals. The presence of an isosbestic point during the reaction suggests the reaction to be an equilibrium process. Figure 2.9 illustrates a typical equilibrium process. Estimation of other thermodynamic data (enthalpy and entropy) is also relatively straight forward [60].

Most metalloporphyrins are labile to axial substitution. However, the degree of substitution may vary depending on the metal, the nature of the

porphyrin macrocycle and the ligand itself. In general, axial substitution can be described by the following.

$$MP + L \rightleftharpoons MPL \qquad (2.12)$$

$$MPL + L \rightleftharpoons MPL_2 \qquad (2.13)$$

$$MP + 2\,L \rightleftharpoons MPL_2 \qquad (2.14)$$

Kinetic and thermodynamic data can be calculated following the procedure discussed above. In an ideal situation, if the stepwise substitution described by Reactions 2.12 and 2.13 is in progress the appearance of two isosbestic points - each being more conspicuous than the other depending on which substitution step is prevalent at the time of observation - is expected. On the other hand, the formation of mono- and bis- complexes through one step substitution reactions (reactions (2.12) and (2.14)) is accompanied by the appearance of one isosbestic point; however, spectral data evaluation would suggest the degree of substitution. In some two step ligand binding reactions the precise analysis of data according to the above procedure can be difficult due to overlapping equilibria. A relationship for evaluating such systems has been derived [64].

In thermodynamic studies of ligand binding to amino acid substituted iron porphyrins conducted by Goff et al. [58], it was found that the reaction of cyanide proceeded in a stepwise manner yielding a bis-cyano complex. The calculated K_1 and K_2 values were, $4.25 \times 10^5\ M^{-1}$ and $8.51 \times 10^3\ M^{-1}$ respectively. In contrast, in the same study it was noted that only the overall equilibrium for two-ligand binding was observed with the ligands pyridine, L-histidine and imidazole. The reaction of iron(III) myoglobin and cytochrome *c* with cyanide was a one ligand binding reaction with a K_1 of $2.3 \times 10^8\ M^{-1}$ and $1.2 \times 10^6\ M^{-1}$ respectively [65].

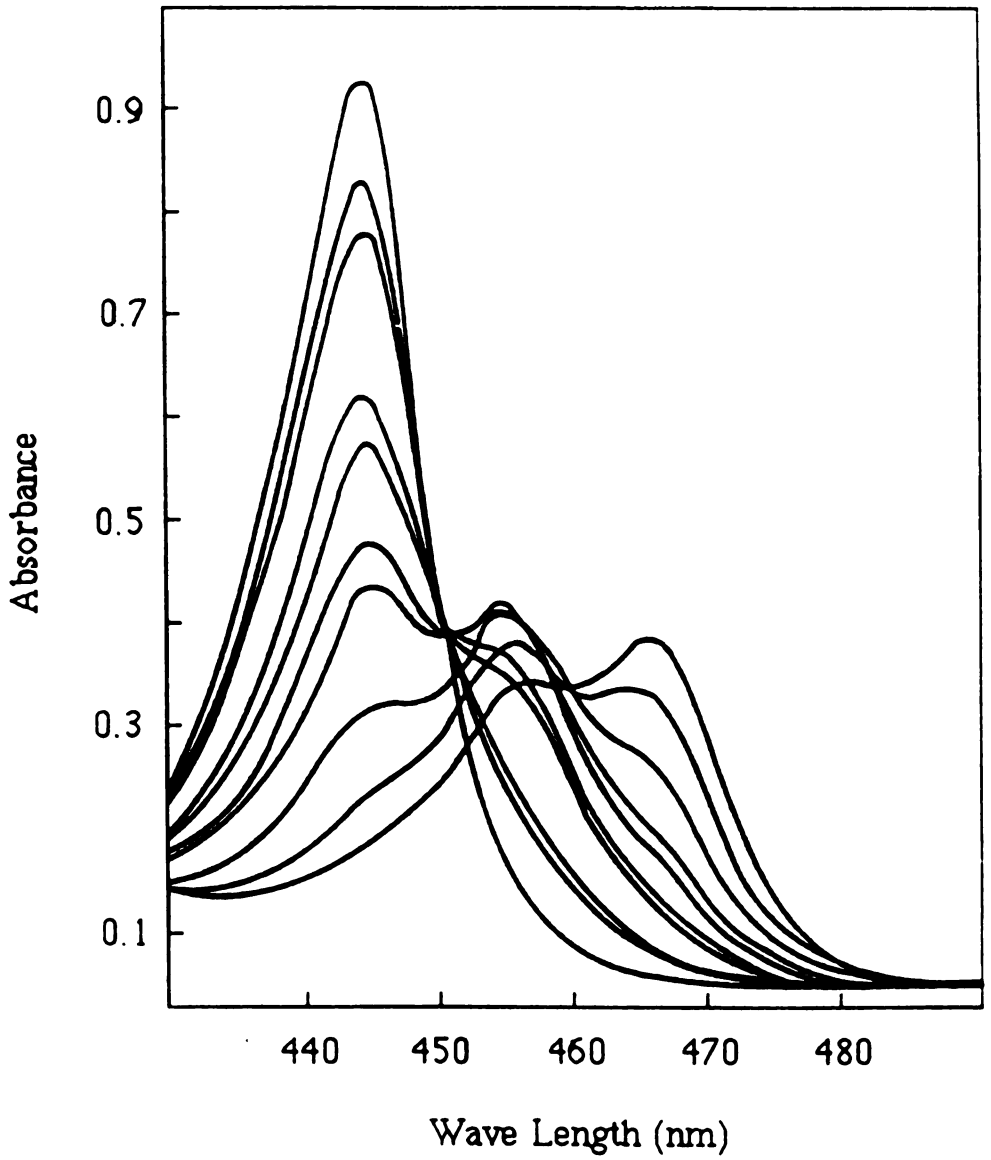

Figure 2.8 [57] Spectrophotometric titrations of Cr(III)TPPS (TPPS = meso-tetra(p-sulfanatophenyl)) with pyridine. The reaction of pyridine with Cr(III)TPPS progressively shifts the absorption maxima to longer wave lengths. Isosbestic points are observed at 451 nm and 458 nm. The presence of two isosbestic points suggests possibility of three species in equilibrium with each other.

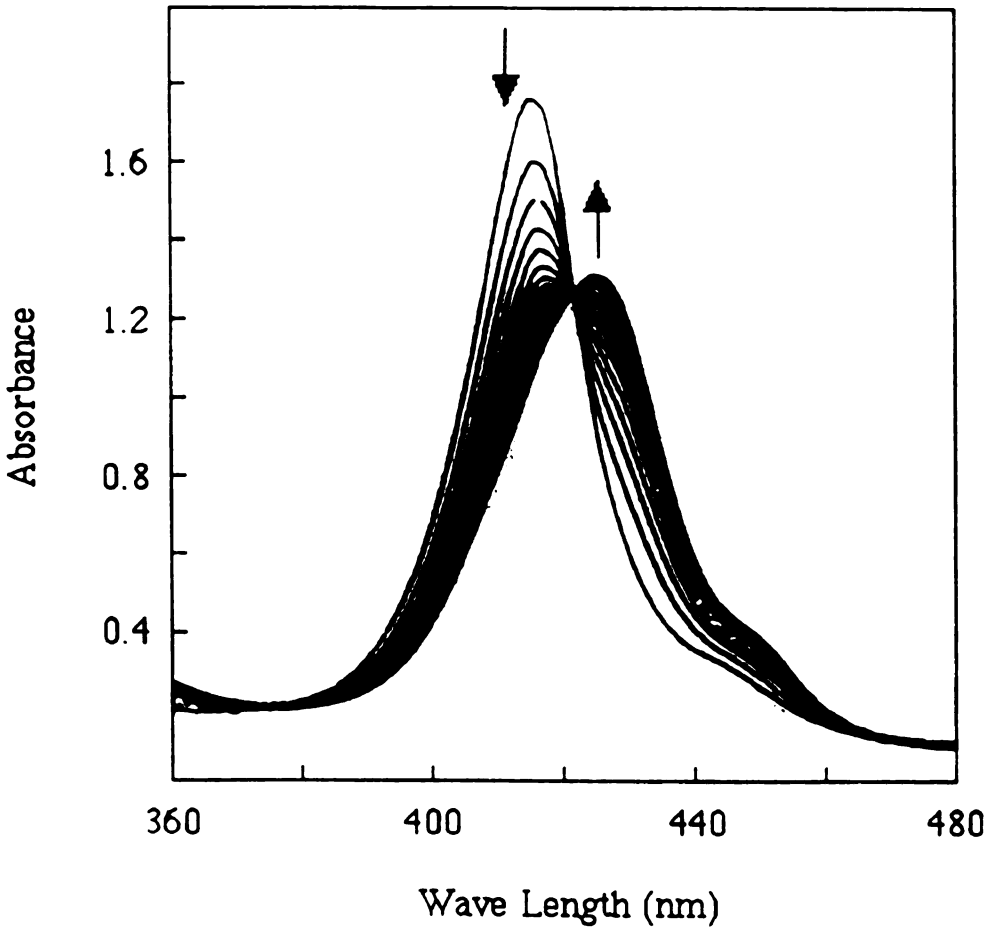

Figure 2.9 [35a] Spectral changes occuring during autoreduction of TPPFe(III)$(CN)_2$ to TPPFe(II)$(CN)_2$. The precence of an isosbestic point suggests an equilibrium reaction. TPP=tetraphenylporphine.

A highly exothermic reaction with a significantly high value for K_1 was observed with cyanide ion displacement of a single dipeptide histidine ligand of dipeptide substituted iron(II) 2,4-bis(cysteinylhistidine)-mesoporphyrin at pH 6.5 [58]. This may be explained by a favorable combination of σ-donor and π-acceptor metal ligand interaction enforced by the protonation of the imidazole group in the displaced dipeptide side chain.

The effect of the porphyrin macrocycle on the stability of complexes is exemplified by the following. Leipoldt et al. [61] compared the stability constants of both $Cr(III)P(H_2O)(NCS)^{4+}$ (P = meso-tetra(4-N-methylporphine)) and $Cr(III)TPPS(H_2O)(NCS)^{4-}$ (TPPS = meso-tetra(p-sulfanatophenyl)) porphyrin complexes to the stability constant of $Cr(III)(H_2O)_5(NCS)^{2+}$ and noted a drastic reduction in stability of the porphyrin complexes (approximately a seventy fold reduction). It is reasonable to argue that this reduction is due to the higher electron density imposed on the metal by the highly conjugated porphyrin molecule. Electron donating groups such as CN^- and NCS^- are less stable under these conditions. It is expected that the presence of highly electron withdrawing groups at the periphery of the macrocycle would enhance the stability of these porphyrin complexes by dispersing the electron density concentrated on the metal. The stability constant for $Cr(III)P(OH)(CN)^{3+}$ was found to be 10^4 times greater than that for $CrP(OH)(NCS)^{3+}$. The strength of the cyanide complex is attributed to the strong s-bonding character of cyanide ligands. The stability constants of Rh(III)TPPS(SCN) ($K = 39\ M^{-1}$) and Rh(III)TPPS(CN) ($K = 1880\ M^{-1}$) also reflect the stronger bonding ability of the cyanide ligand [66].

2.3 Development of Optical Sensory Devises Using Molecular Probes Confined in Polymeric Matrices

Development of the sol-gel process has paved the way to processing novel materials having a variety of chemical and physical properties suitable to many applications including optical sensors. The sol-gel technique, in addition to providing stable, transparent and porous material, offers a multitude of modifying techniques that may be necessary to sustain foreign molecular probes in good optical condition. The porous matrix should be such that it accommodates the probe molecules with ideally no excretion but at the same time allowing maximum access for detectable species to the immobilized probe through favorable diffusion properties that minimize barriers to mass transport. The sol-gel process allows adjustment of diffusion properties through structural modifications. The sol-gel process and its traits were discussed extensively in section 2.1.

Some likely candidates to be used as molecular probes include, (I) enzymes and other proteins that possess high specificity for binding of detectable species such as substrates, inhibitors or related molecules, (II) dye molecules such as pyrenene derivatives that are extremely sensitive to the environment (solute-solvent interactions), (III) metalloporphyrins or like macrocyclic compounds with metal centers that are susceptible to axial binding by ligands such as cyanide, carbon monoxide, halides and pyridine.

All the probe molecules named above have a characteristic optical absorption spectrum that is sensitive to their bound species or the immediate environment. Retention of these properties once immobilized within the supporting matrix is critical to the construction of a sensing devise. Generally, probe molecules react with target species or respond to the environment rapidly in solution. Physical and chemical effects

imparted by the matrix may increase the equilibrium time. The dynamic response range of the probe molecule to the analyte can be reduced drastically. It follows that these molecules ideally should have no interactions - that may impede their sensitivity - with the elements of the matrix or the carrier solvent; electronic or otherwise. However, it should be mentioned that, in the case of metalloporphyrins in solution, researchers have noted instances where interactions at sites remote to the active center of the probe have favored reactions and their reactivity (see the preceding section).

In principle, thin film like porous support matrices should favor faster response time in the sensing process. The sol-gel process is easily adapted to processing supported thin films with few modifications. The thickness of the films is also adjustable and can help when probe molecules with lower absorption cross sections are used. These material may also have the ability to act as optical filters that absorb light at specific wave lengths that cause photodegradation of probe molecules [67].

An ideal optical sensor should have the capability to reflect the fluctuations in analyte concentration continuously; i.e., the optical probe should interact with the analyte in a reversible manner for long periods of time. However, most colorimetric and florimetric reactions are irreversible because resulting products are tight binding complexes. A pragmatic solution that avoids such problems is the construction of cheap, single use and recyclable test kits. Sol-gel material and the process is well suited for the manufacture of economically viable and environmentally friendly polymer matrix supports.

Primarily, there are three methods to incorporate probe molecules within the matrix.

(I) ***Entrapment:*** The probe molecule can be entrapped within the porous matrix by dissolving it in the sol-gel solution prior to spin casting or any other processing technique that is preferred. This method requires the probe molecule to be sufficiently soluble in the polymeric sol-gel solution such that a functional amount would be available within the matrix to react with a corresponding detectable species. Stability of probe molecules in polymeric sol-gel solutions should be considered. Enzymes and other proteins are susceptible to denaturation by various solvents such as ethanol used to attain homogeneity in sol-gel mixtures. Aggregation resulting from unfavorable pH conditions and/or unfavorable ionic character of the solution may retard the sensitivity. Metalloporphyrins are subject to similar constraints and a detailed discussion precedes this section.

(II) ***Covalent immobilization:*** Probe molecules can be covalently linked to the polymer matrix through chelating ligands such as organic acid groups that are attached at the periphery of the probe molecule. Derivatives of metalloporphyrins are prime candidates for this kind of immobilization. However, steric effects of the bulky probe molecules may substantially hinder such substitution reactions.

(III) ***Adsorption:*** Bulky probe molecules like enzymes and other proteins may be physically adsorbed on to polymer matrices through hydrophobic interactions. However, the method is likely to be less stable. A more effective method would be to chemically adsorb coupling agents doped with reactive chromophores to the polymer matrix. This application is especially suited for sol-gel processed material since the sol-gel network (TiO_2, SiO_2 etc.) is very responsive to silanol type bonding with silicon coupling agents.

Both entrapment and covalent immobilization require the probe molecule to be introduced at the preparatory stages of the polymer. High temperature synthesis techniques common to more conventional polymers can be detrimental to the stability of many potential probe molecules. The ability of the sol-gel method to process stable porous matrices at or near room temperature circumvents fabrication problems posed by thermal degradation to probe molecules.

More conventional matrix supports have been used to construct sensory devises applying the same principle. Some of them are presented below since the fabrication schemes, especially of molecular probes, are tantamount to the work presented herein. Examples for the successful application of the sol-gel process in sensor technology follows.

Narayanaswamy et al. [68] devised a detection system for fluoride in a flowing stream by use of a colorimetric reagent immobilized in a polymer matrix in combination with a bifurcated fiber-optic system that shines and then collects reflected light. It is known that cerium(III)-alizarin complexone, a derivative of anthraquinone, forms a ternary complex with fluoride and that the reaction is highlighted by a color change from wine-red to blue. Cerium(III)-alizarin complexone was immobilized in amberlite XAD-2 porous polymer beads by adsorption. Hydrophobic interactions between the polymer and the nonpolar region of the complex enabled easy immobilization. A linear response of the reflectance measurement was obtained for 0.16 - 0.95 mM fluoride at a pH of 4.1. The reported response time was approximately 12 min.

8-hydroxypyrene-1,3,6-trisulfonic acid (HPTS) participate in acid base equilibria and its fluorescence emission is extremely receptive to the solvent pH. A pH sensor based on the measurement of the fluorescence

emission intensity of HPTS was prepared by Shufang et al. [69]. The sensory device was crafted such that the reagent is delivered slowly by a mass of ethylene-vinyl acetate (EVA) copolymers upon contact with aqueous solution. The ratio of the fluorescence emission intensities at 515 nm from excitation at 405 nm and 450 nm gave a dynamic range from pH 5.5 to pH 8 with minimum precision of $\pm$ 0.07 pH units. The controlled-release technique utilized here is reported to be effective for at least three months.

The relative magnitude of fluorescent energy transfer corresponding to the proximity of a donor and an acceptor was used as an optical parameter to measure the ionic strength of aqueous solutions [70]. Even though, the reagents used in this system were confined behind a dialysis membrane, not within a matrix, the underlying chemistry in operation is instructive. At low ionic strength, fluorescein-labeled dextran and sulforhodamine-labeled polyethyleneimine associate. The resulting proximity of the donor (sulforhodamine) and the acceptor (fluorescein) enables them to transfer fluorescent energy. The fluorescence maximum of fluorescein located at 520 nm (excitation at 493 nm) is enhanced in this configuration and it drops off upon dissociation of the carriers when the ionic strength of the solution is increased. Calibrations of the optical measurement with the log of ionic strength proved to be fairly linear.

The analytical potential of confined electrochromic dyes for the measurement of the electric field in an electrolyte solution was demonstrated by Opitz et al. [71]. The wave length shift of the emission spectrum of *trans* -4-[4-(dodecyloxy)phenylethenyl]-N-methylpyridinium iodide, confined within multilayers of ultraviolet-polymerized pentacosa-

diynoic acid, depended linearly on the applied field strength up to 1.3 x 10^6 Vcm^{-1}.

An optical pH sensor was constructed using acid-base equilibrium characteristics of the dye Congo Red [72]. The dye was immobilized within the porous structure of a hydrolyzed cellulose acetate film supported on microscope slides. The immobilization was achieved by immersing the dried polymer film in a hot dye bath. Chemical interactions between both amine and azo groups of the dye and the hydroxy groups of the cellulose film are thought to instigate the immobilization of the dye. The optical response of Congo Red to variations in pH measured in transmission mode indicated a dynamic range of 4 pH units.

Ellerby et al. [73] were successful in encapsulating proteins in porous silicate glasses prepared under mild conditions - characteristic of the sol-gel process - such that the proteins retained their characteristic reactivities and spectroscopic properties. Proteins are extremely susceptible to denaturation caused by solvent types and conditions. For instance solvents like alcohol and acidic conditions can cause protein denaturation and aggregation. Both acid catalysis and alcohol are extensively used in the sol-gel process. However, a wide variety of avenues are available for the modification of the process such that the conditions are suitable to analytical reagents. Ellerby et al. avoided the use of alcohol and also adjusted the pH of the product mixture resulting from HCl-catalyzed hydrolysis of tetramethyl-orthosilicate (see Section 2.1) to above 5.0 prior to the addition of protein. The modification apparently circumvented acid denaturation of proteins or aggregation of proteins or both. The following were successfully performed with the encapsulated proteins; copper-zinc superoxide dismutase was demetallated and then remetallated,

ferricytochrome *c* was reduced and then reoxidized and met myoglobin was reduced to deoxy myoglobin and then reacted either with dioxygen to make oxy myoglobin or with carbon monoxide to make carbonyl myoglobin. The experiments demonstrated that metallo-organic sol-gel networks are capable of hosting biochemically active macromolecules and that such systems have the potential for use as biosensors.

The absorption-energy-transfer-emission (AETE) process demonstrated by lanthanide cryptates was used to detect the presence of molecules with light harvesting centers (LHC) by encapsulating cryptate complexes within sol-gel processed titanium thin films [74]. The coordination of derivatives of β-diketonates and carboxylic acids to lanthanide cryptates can greatly enhance the emission intensity of the lanthanide center. This occurs as a result of energy transfer from the light harvesting center of the ligand to the lanthanide via intermolecular interactions. Dulebohn et al. [74] entrapped both the native Eu^{+3} and a cryptate complex of Eu^{+3} in a sol-gel derived titanium based thin film and they were able to detect the presence of the salts of benzoic acid and 4-*tert*-butylbenzoic acid in aqueous solution. The entrapment was accomplished by dissolving the water soluble cryptate complex in the water that is added to hydrolyze the alkoxide precursor. The emission intensity calibrated against the salt LHC concentration was linear for both the cryptate and the native Eu^{+3} complex in the range studied.

3 Experimental

3.1 Titanium Metallo-Organic films Produced by Sol-Gel Processing

3.1.1 Materials and Instrumentation

Titanium(IV)isopropoxide and carboxylic acids were purchased from Aldrich Chemical Company and used with no further purification. Water deionized with a resistance of 18 Mohm was used. VWR precleaned microscope slides (3 x 1", 1.2 mm) were used as substrates for films and they were cleaned prior to usage. A Scientific Industries Vortex Genie 2 stirrer was used to agitate the reaction mixtures. The reaction mixtures were contained in Research Products International Corp. screw-top liquid scintillation glass vials. An International Clinical Centrifuge (model CL 26802 M) was used for spin-casting films. The film thicknesses were measured on a DEKTAK IIA profilometer.

3.1.2 Processing

(I) ***Sols:*** Titanium(IV)isopropoxide was added to the carboxylic acid placed in a screw-top vial. The mixture was stirred vigorously. Then water was added to the resulting solution and the mixture was stirred vigorously as before. When carboxylic acids in solid form were used they were added to titanium(IV)isopropoxide placed in screw-top vials and were melted at 60°C and stirred to form homogeneous solutions.

(II) ***Films:*** Films were made by spin-casting solutions on microscope slides taped to the clinical centrifuge. The coating solution

(film solution) was placed on the microscope slide using a Pasteur pipette and then the solution was spread evenly over the slide using the same pipette. The films were cast immediately to remove excess solution. Each film was cast individually for three minutes and then stored in a dust free chamber for observation. Casting was carried out in a ventilated environment.

Film thickness measurements: Films cast on microscope slides were etched using a fine blade at the center of the slide perpendicular to the longer dimension of the slide. The film surface was scanned with the DEKTAK IIA profilometer along the longer dimension of the slide across the "micro crevice" indented by the blade. Thickness was obtained by measuring the profile of the crevice generated by the instrument.

3.2 Encapsulation of the Metalloporphyrin Within the Porous Film

3.2.1 Materials and Instrumentation

Films modified by valeric acid at $R_a = 9$ were used to encapsulate the metalloporphyrin. The used R_w was 1.5. The films were supported on microscope slides cut to fit 1 x 1 cm cuvettes. The cast films were dried using a Master Heat Gun. The metalloporphyrin was tetrakis-(pentafluorophenyl)porphineFe(III)Cl, (PFPP), and was synthesized and provided by Chang [75]. Absorbance measurements were taken in a Perkin-Elmer Lambda 3A UV/VIS Spectrophotometer. Fisher Scientific 1 x 1 cm disposable polystyrene cuvettes were used to hold the films (supported on slides) vertically across the UV/VIS beam path. Spectra

were recorded on a Perkin-Elmer R 100A Recorder. Absolute ethanol was purchased from the Quantum Chemical Corporation.

3.2.2 Encapsulation of the Metalloporphyrin

The film solution composition is given in Table 3.1. The preparation of the solutions was as follows; first, PFPP was dissolved in valeric acid and then titanium(IV)isopropoxide was added to the porphyrin solution. After a few seconds of vigorous stirring, water was added and the mixture was stirred again. Finally ethanol was added to the mixture. The effect of added ethanol on encapsulated PFPP stability was studied. The range studied was between R_e values (the molar ratio, ethanol to alkoxide) of 10 and 40.

Table 3.1 Composition of the PFPP incorporated film solution.

Component	Molar Ratio (R^*)
PFPP	$R_p = 0.008$
Valeric Acid	$R_a = 9.0$
Water	$R_w = 1.5$
Ethanol	N/A

* Molar ratio with respect to titanium (IV)isopropoxide
PFPP: tetrakis(pentafluorophenyl)porphine Fe(III)Cl

The film solutions were aged for at least 24 hr prior to casting but were used within one week. The film solution were cast on cut microscope slides for 3 min. and the cast films were dried for 1 min. with a heater gun at 200°C, primarily to drive off excess valeric acid which possesses an unpleasant odor. Both casting and drying were carried out in a ventilated environment.

The stability of PFPP encapsulated within the polymer matrix was studied using UV/VIS absorbance spectroscopy. Cast films supported on cut slides were placed vertically inside polystyrene cuvettes in pairs. The pair was placed against the opposite walls of the cuvette such that both films were oriented toward the cavity of the cuvette and not the wall. The cuvette was placed in the spectrophotometer cell compartment such that the film surfaces were perpendicular to the beam path. In order to obtain porphyrin absorbance spectra that were as precise as possible, a reference cell of the same configuration, but with films free of porphyrin was used in the reference compartment of the double beam spectrophotometer.

3.3 The Cyanide Sensor

3.3.1 Materials and Instrumentation

Films modified by valeric acid at $R_a = 9$ and by ethanol at $R_e = 40$ were used to encapsulate the metalloporphyrin. R_w was 1.5. The films were cast and then dried as described in section 3.2.1. The films were supported on microscope slides cut to fit 1 x 1 cm cuvettes. The cast films were dried using a Master Heat Gun. The metalloporphyrin was tetrakis-(pentafluorophenyl)porphineFe(III)Cl, (PFPP), and was synthesized and provided by Chang [75]. Absorbance measurements were taken in a Perkin-Elmer Lambda 3A UV/VIS Spectrophotometer. Fisher Scientific 1 x 1 cm disposable polystyrene cuvettes were used to hold the slide-supported films vertically across the UV/VIS beam path. Spectra were recorded on a Perkin-Elmer R 100A Recorder.

3.3.2 Construction of the Cyanide Sensor

The configuration of the sensor cell is given in Figure 3.1. The glass substrates supporting the films were placed firmly against the cuvette walls by wetting the contact surfaces. Two films were used in order to increase the signal to noise ratio. Also, background spectral interferences were minimized by using a reference cell of the same configuration with films free of PFPP in the reference compartment of the double beam spectrophotometer.

All films used in this experiment were stored in a dark environment prior to usage; however, they were exposed to room conditions. The films were soaked in water for about 15 min., immediately preceding the contact with cyanide solutions, to avoid contributions from spectral changes due to water.

The experimental procedure was as follows. Both the active cell and the reference cell were placed in their respective compartments. Then 3 ml of an aqueous cyanide solution of known concentration was introduced to the empty active cell and timing was commenced immediately. After 15 min. of elapsed time the absorbance intensities at 410 nm and 430 nm were recorded. The ratio of absorbance at 430 nm to absorbance at 410 nm was recorded for cyanide concentrations ranging from 400 ppb to 25,000 ppm. From the time the active cell was placed in the cell compartment to the time the measurement was taken the incident light beam was blocked as a precautionary measure against photodecomposition of PFPP.

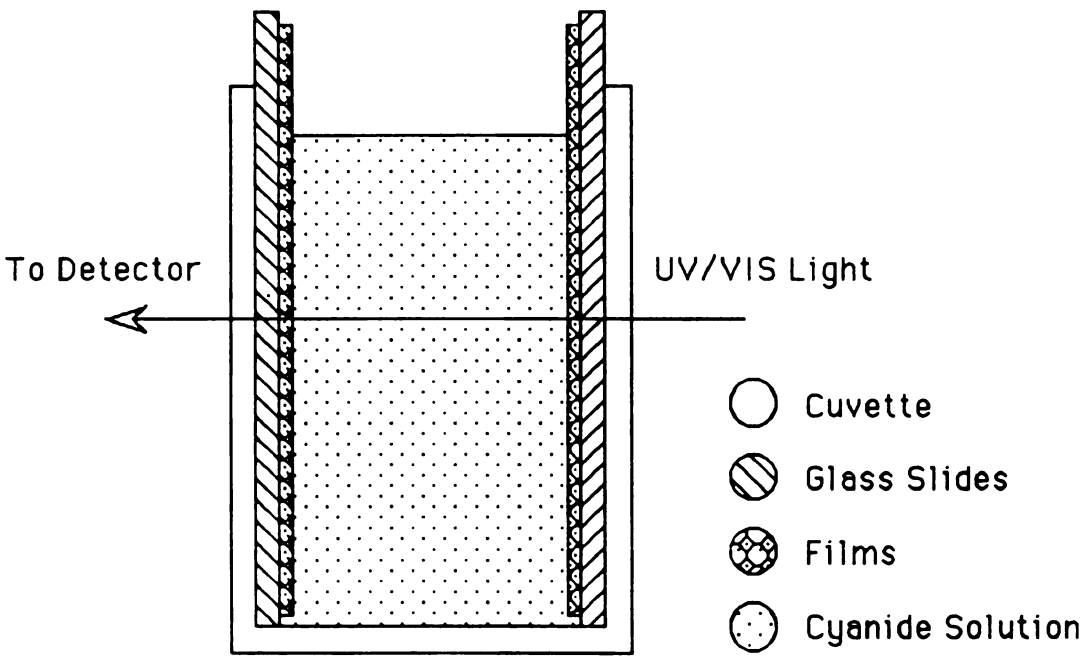

Figure 3.1 Cell Configuration.

4 Results and Discussion

4.1 Titanium Metallo-Organic films Produced by Sol-Gel Processing

Controlled hydrolysis of alkoxide precursors is the key to making thin films using the sol-gel process (see section 2.1.5). In the work presented herein, the feasibility of a series of carboxylic acids as hydrolysis-controlling reagents in a titanium based sol-gel system and also the overall effect of the exerted control on film quality were investigated. The series of carboxylic acids studied included, acetic acid, propionic acid, butyric acid, valeric acid, hexanoic acid, octanoic acid, lauric acid and myristic acid. In addition, the effect of the relative amount of carboxylic acid introduced to the sol-gel system on film quality was studied. The relative amount of carboxylic acid used was measured in terms of the molar ratio between the acid and the titanium alkoxide (R_a) and the ratio ranged from 3 to 10. The molar ratio of water to alkoxide (R_w) was 1.5.

(I) *Sols:* The reactions between the titanium alkoxide and acids, in each case, were exothermic and yielded a range of colorless to yellow homogeneous and transparent solutions depending on the acid. Upon the addition of water to the reaction mixtures of acetic and propionic acid, an immediate phase separation in the form of a white precipitate was observed throughout the range of R_a values studied. The formation of the white precipitate and therefore the phase separation was confined to a limited volume that somewhat reflected the volume of the added water. White precipitates observed in these systems are insoluble hydroxides that form as a result of the facile substitution of alkoxy groups of alkoxides by hydroxy

groups. An instantaneous heterogeneous reaction facilitated by the bulk introduction of water to the modified precursor may have caused the phase separation. Similar effects were observed by Kamia [7].

When the reaction mixtures of the propionic acid system, at high R_a values, were stirred vigorously the precipitate dissolved in the bulk solution readily and a homogeneous solution resulted. At lower R_a values the solids required more time and stirring for dissolution. However, agitation of the acetic acid system initiated a catalytic effect that formed an insoluble bulk white precipitate. Both butyric and valeric acids yielded a solid only at low R_a values. The solids dissolved easily. At higher R_a values the added water was not miscible in the bulk solution and remained as a separate suspended liquid phase until the system was stirred. In the reaction mixtures where hexanoic and octanoic acids were incorporated only a separate suspended liquid phase was observed upon the addition of water throughout the range of R_a values studied . The suspension easily dissipated upon stirring. All acids, except acetic acid, gave colorless to yellow transparent and homogeneous solutions upon vigorous stirring.

Bradley et al. [13] observed that the reaction rate of normal titanium alkoxides decreases with the increase of the length or the bulkiness of alkoxy groups. Alkoxy groups having non primary structures also contribute to slower reaction rates. Steric effects of lengthy or bulky groups tend to hinder the susceptibility of the titanium atom to nucleophilic attack by potential reagents. The experiments with the modified reagents also seem to conform this trend. As the length of the substituting carboxylic acid chain and also the relative amount of carboxylic acid added are increased, the occurrence of precipitation upon the addition of water gradually decreased. At the same time a progressive increase in the

appearance of the unreacted aqueous suspension is observed. Both these trends suggests that titanium alkoxides substituted with carboxylic acids of shorter chain length are relatively more reactive compared to those substituted with acids of longer chain length. Fast reactions were reflected by the instantaneous precipitation of the white hydroxide suspension. Conversely, the appearance of an unreacted aqueous suspension was reflective of the resistance of the modified species to hydrolysis.

Alkoxy groups are more facile; thus, coordination sites occupied by them are much more susceptible to hydrolysis than are sites occupied by carboxy ligands. Substitution of some of the coordination sites by carboxy ligands does not entirely prevent the hydrolysis of the sites occupied by the remaining alkoxy groups. Carboxy ligands or any other related chelating agents only lower the rate and extent of hydrolysis. They do so by occupying some of the coordination sites through less hydrolyzable bonds or by other physically restrictive impedances such as steric effects that effectively hinder the hydrolysis of alkoxy groups. Note that within an environment where external heat or pressure is not applied, it is unlikely that more than two of the alkoxy groups on the titanium(IV)alkoxide are replaced by acid groups [76]; i.e., atleast two hydrolyzable sites are available in each alkoxide molecule. Then, it is plausible to rationalize that, in our scheme of reactions, the steric effects of longer carboxy ligands were responsible for the reduction in the rate of hydrolysis. Acetic acid, in agreement with these results that produced a completely insoluble hydroxide, is expected to offer the least resistance to hydrolysis of the remaining alkoxy groups.

Earlier work [76] established that the extent of substitution by carboxylic acids is proportional to the R_a value. Therefore, at low R_a

values a low extent of substitution is expected. The word extent is used in the following context; the amount of alkoxide molecules subjected to substitution. That is, at higher R_a values more and more of the alkoxide molecules attain a level of saturation governed by the reaction conditions (temperature, pressure etc.). At ambient conditions it is unlikely that more than two molecules of acid would react with one molecule of alkoxide. It follows that the reactivity of modified alkoxide precursors toward hydrolysis should be lower at higher R_a values, since then, many of the sites otherwise available for hydrolysis would be occupied by more stable carboxy ligands. In the case of propionic, butyric and valeric acids, the tendency toward hydroxide precipitation decreased as the R_a value was increased. The observed trend is in compliance with the above argument.

Dilution of the alkoxide may also be a factor that contributes toward lower rates of hydrolysis at high R_a values. At higher R_a values, excess carboxylic acid dilutes the modified precursor significantly. Consequently, contact between water and alkoxide is minimized.

(II) ***Films:*** Films were characterized qualitatively in terms of optical transparency, brittleness reflected by cracks in the film structure and adherence to the substrate. Films that demonstrated a tendency to crack were considered unstable. Optically transparent films with excellent adhesion properties and structural integrity (no cracking) were considered stable.

A tangible series of results, in terms of film quality, were obtained using propionic, butyric and valeric acid. The results are tabulated in Table 4.1 (note that the classification denoted "time before cracking" is an approximate measurement of the time unstable films were observed to commence cracking, counted immediately after three minutes of casting).

Table 4.1 Dependence of film stability on composition.

a. Propionic acid, $R_w = 1.5$

R_a	$R_{w/a}$	Stability Time before cracking
3.0	0.51	0
4.0	0.38	0
5.2	0.29	0
6.0	0.25	0
7.0	0.22	0
8.0	0.19	0
9.0	0.17	0
10.0	0.15	30 min

b. Butyric acid, $R_w = 1.5$

R_a	$R_{w/a}$	Stability Time before cracking
3.0	0.51	5 min
4.0	0.38	10 min
5.2	0.29	30 min
6.0	0.25	12 hr
7.0	0.22	12 hr
8.0	0.19	12 hr
9.0	0.17	Stable
10.0	0.15	Stable

Table 4.1 is continued on the following page.

Table 4.1 cont'n.

c. Valeric acid, $R_w = 1.5$

R_a	$R_{w/a}$	Stability Time before cracking
3.0	0.51	20 min
4.0	0.38	40 min
5.2	0.29	Stable
6.0	0.25	Stable
7.0	0.22	Stable
8.0	0.19	Stable
9.0	0.17	Stable
10.0	0.15	Stable

The classification denoted "time before cracking" is an approximate measurement of the time unstable films were observed to commence cracking, counted immediately after three minutes of casting.

R_a: molar ratio of acid to alkoxide
R_w: molar ratio of water to alkoxide
$R_{w/a}$: molar ratio of water to acid

The series of films made from solutions containing precursors modified by valeric acid was the most flexible. The flexibility decreased drastically from valeric acid to butyric acid to propionic acid. Solutions that contained polymeric systems derivatized by hexanoic acid and octanoic acid possessed extremely poor adhesion properties and they failed to produce quality films.

Earlier in this discussion it was established that carboxylic acids of longer chain length and also higher R_a values contribute to reduced rates of hydrolysis. Evidently, the reduced rates of hydrolysis can be correlated to improved film quality. Higher R_a values of both butyric and valeric acid produce stable films. The data show that the films approach stability in ascending order of R_a, most likely reflecting the gradual decrease in the rate and the extent of hydrolysis of the alkoxide derivative. Even though propionic acid does not produce stable films, the extent of cracking decreases as the R_a is increased and the trend is in general agreement with the other two acids. The widest range of stable films was produced by valeric acid film solutions followed by butyric acid. The trend is in accordance with slower rates and lower extents of hydrolysis resulting from increased steric effects of the longer chain carboxylic acid.

The impedance of hydrolysis by steric effects is expected to be most pronounced in systems modified by hexanoic and octanoic acid. Hydrolysis of the alkoxide initiates the polymerization process that compounds the structure of the sols and subsequently the structure of the films (see section 2.1.4). If hydrolysis is hindered to an extent that only smaller oligomeric units are formed, it is reasonable to conceptualize that such systems would not produce continuous films due to the lack of linear and cross linked matrix formation. The inability of systems modified by hexanoic and

octanoic acids to produce film solutions with good adherence properties seem to suggest that these systems behave in compliance with the reasoning presented above.

One could argue that the higher hydrophobicity of hexanoic and octanoic acid effectively blocks the hydrophilic metal-oxygen-metal coupling between the substrate and the film. As a consequence, good adherence properties could be negated. However, in an experiment in which hydrophobic polystyrene surfaces were coated with the same modified film solutions, the trend in adherence properties were observed to be similar to that on silicate glass substrates. This behavior implies that poor adhesion properties enforced by hydrophobic effects can be discounted as a possible explanation. If hydrophobic effects were important, at least a crude reversal in the trend in coating properties should have occurred. Inadequate polymerization of less hydrolyzable modified precursors seem to be the likely explanation for the exhibited inconsistency in coating properties of film solutions made of longer chain hexanoic and octanoic acids.

Following the reaction between the alkoxide and the carboxylic acid, the excess acid and the alcohol byproduct may react to form the corresponding ester according to the following reaction [77];

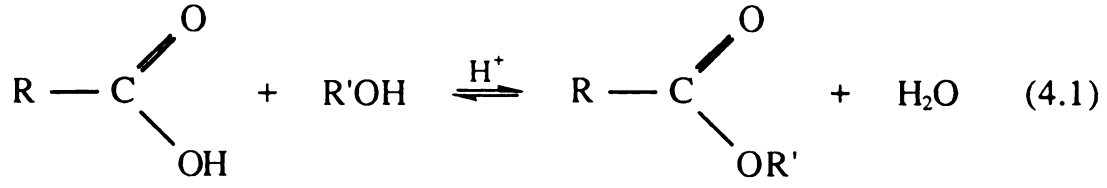

(4.1)

The reaction is usually catalyzed by mineral acids. However, titanium can also exert a catalytic effect for the reaction. Earlier work [78] shows evidence for the formation of esters in a similar system. The water

generated by the esterification reaction may induce hydrolysis and subsequent polymerization prior to the external addition of water. The inadequacy of the water so generated for hydrolyzing the modified precursors was tested. The results tabulated in Table 4.2 demonstrate that the internally generated water alone is not capable of inducing the formation of a polymer matrix with the structural integrity necessary to remain stable as a uniform film. Variation of R_w over the range from 1 to 5 has no effect on film quality at a macroscopic level. Nevertheless, the importance of additional water is clear.

It was observed that longer chain carboxylic acids reacted at elevated temperatures in combination with shorter chain carboxylic acids are capable of stabilizing otherwise unstable films. The series of film solutions modified by propionic acid was preferred to study the stabilizing effect since the films they produced were not stable through the range. Lauric and myristic were the longer chain carboxylic acids utilized in this experiment. The process sequence was as follows; The longer chain carboxylic acid, $R_a = 0.36$ for lauric acid and $R_a = 0.31$ for myristic acid, was added to the titanium(IV)alkoxide placed in a screw-top vial. The heterogeneous mixture was heated at 60°C until the solid melted to form a homogeneous solution. Then the shorter chain carboxylic acid was added to the well stirred mixture and was stirred again. This step was followed by the introduction of water, $R_w = 1.5$, and thorough stirring. The results are tabulated in Table 4.3.

At $R_a = 8$, without the incorporation of a longer chain carboxylic acid, the propionic acid film solution produced a film in which cracking was observed upon casting for three minutes. However, the introduction of a small amount of lauric or myristic acid resulted in a film in which

Table 4.2 Dependence of film stability on composition.

Butyric acid, $R_a = 9.8$

R_w	$R_{w/a}$	Stability Time before cracking
0.0	0.00	24 hr
1.0	0.10	Stable
2.0	0.20	Stable
3.0	0.31	Stable
4.0	0.41	Stable
5.0	0.51	Stable

The classification denoted "time before cracking" is an approximate measurement of the time unstable films were observed to commence cracking, counted immediately after three minutes of casting.

R_a: molar ratio of acid to alkoxide
R_w: molar ratio of water to alkoxide
$R_{w/a}$: molar ratio of water to acid

Table 4.3 The dependence of film stability on added long chain carboxylic acids.

Components in Film Solution	Composition R_a	Stability Time Before Cracking
Propionic Acid Lauric Acid	8 0.0	0
Propionic Acid Myristic Acid	8 0.0	0
Propionic Acid Lauric Acid	8 0.36	24 hr
Propionic Acid Myristic Acid	8 0.31	24 hr
Propionic Acid Lauric Acid	16 0.36	Stable
Propionic Acid Myristic Acid	16 0.31	Stable

The classification denoted "time before cracking" is an approximate measurement of the time unstable films were observed to commence cracking, counted immediately after three minutes of casting.

R_w, (molar ratio of water to alkoxide): 1.5

R_a: molar ratio of acid to alkoxide

cracking was observed much later. The effect was much more pronounced at R_a = 16, in which case the addition of either lauric or myristic acid enabled the production of a stable film. The stabilizing effect of lauric and myristic acids was just as effective in low R_a films of both butyric and valeric acids.

Preceding arguments established that precursors modified by shorter chain length carboxylic acids were susceptible to faster and greater hydrolysis compared to that modified by relatively longer chain carboxylic acids. Accordingly, controlled hydrolysis was correlated to the formation of stable films. The observations just presented seem to further confirm the argument. Annexation of a small amount of lauric or myristic acid to a unstable shorter chain system produces a stable film. The stability of these films is likely due to the disposition of the system to produce polymer matrices of favorable structural integrity at low rates and low extents of hydrolysis. Lower rates and extents of hydrolysis upon annexation of longer chain lauric or myristic acids to shorter chain systems is expected due to increased steric effects.

The control imparted by shorter chain carboxylic acids or low R_a values or both on rates and extents of hydrolysis can be relatively low in magnitude leading to excessively cross linked polymer matrices. Relaxation of the polymer strands along with the solvent evaporation that accompanies casting and drying of films is made difficult by the structural rigidity of excessively cross linked matrices. Such systems are likely to yield brittle layers that crack upon drying as those conceivably produced by film solutions modified by propionic acid and others at low R_a values. Modification of the alkoxide precursor by longer chain carboxylic acids that reduce the extent of hydrolysis and thus cross linking, should allow

easier relaxation for the polymer strands leading to stable and continuous films. This behavior was strikingly noticeable in the stabilizing effect demonstrated by both lauric and myristic acids on unstable propionic acid systems. Comparison of properties of films produced by solutions modified by propionic acid, butyric acid and valeric acid conveys that film stability is achieved by controlled hydrolysis. In addition, longer chains are more elastic in nature. Elasticity provides further flexibility to the matrix and helps the formation of crack free films.

Stability of the films to external elements such as solvents and varied pH conditions was tested using a valeric acid film (R_a = 9). The film was insoluble in water and organic solvents (methanol, acetone, acetonitrile, benzene, xylene, chloroform and carbon tetrachloride). The effect of solutions (HCl/NaOH) with pH ranging from 1 to 10 on films is tabulated in Table 4.4.

Film thickness measurements are tabulated in Table 4.5. The R_a value of the film solutions was 10 in all cases. Thickness of the films decreased in the following order; propionic acid > butyric acid > valeric acid. These measurements also suggests that extensive polymerization initiated by less controlled hydrolysis is prevalent in films modified by propionic acid. The opportunity to polymerize extensively can lead to thick matrices held by cross linking.

It was noted that comparisons made solely based on the film thicknesses measured at a constant R_a value - in comparing propionic, butyric and valeric acids - would lead to erroneous conclusions. This is likely since higher molecular weight acids are accompanied by a volume increase in order to maintain the constant R_a. This in turn increases the total volume of the film solution. Then the added water is diluted in the

Table 4.4 Stability of films in aqueous solutions at different pH values.

Solution pH (HCl/NaOH)	Stability of Films
1	dissolved within 1 hr
4	stable
7	stable
10	etched after 1-2 weeks

Valeric acid films made with a solution at R_a=10 and R_w=1.5 were used in this experiment. The films were immerced in the respective solutions for a period of one month.

R_a: molar ratio of acid to alkoxide
R_w: molar ratio of water to alkoxide

Table 4.5 Film thickness measurements.

Type of Film	Film Thickness A°
Propionic Acid	4900 ± 200
Butyric Acid	2500 ± 200
Valeric Acid	1400 ± 200

Film thicknesses were measured as described in the experimental section. Films made with solutions at R_a=10 and R_w=1.5 were used in this experiment.

R_a: molar ratio of acid to alkoxide
R_w: molar ratio of water to alkoxide

reaction mixture and its access to sites of hydrolysis may be limited. The unavoidable circumstance can effectively reduce the extent of hydrolysis and produce thinner films. The effect progressively increases from propionic to butyric to valeric acid. However, the film thickness measurements presented in Table 4.6 manifests the credibility of the former argument that the progressive reduction in thickness from propionic to valeric acid, at least in part, is due to control of hydrolysis exerted by steric effects. In this experiment the total volume of each film solution was kept constant by using the same volume amounts of alkoxide , acid and water.

The data presented in Table 4.7 compare thickness of valeric acid films at different R_a values. The thickness decreases with increasing R_a. In this case it is possible that both higher R_a and dilution in combination are affecting the desired control. At higher R_a more and more of the alkoxide molecules are substituted by carboxy groups thereby limiting hydrolysis and dilution limits the amount of water available for hydrolysis. Experiments to determine the relative contribution of the two phenomenon were not conducted.

It is conceivable that dilution of the polymer in excess acid can lead to thinner films. However, the trends established in this work suggest that the relative contribution of the bulk dilution towards film thicknesses is quite low in the range experimentally covered. In this range, the reduction in film thickness is accompanied by an improvement in film quality. This is unquestionably a consequence of a chemically induced alteration; thus, a chemical phenomenon.

Table 4.6 Film thickness measurements.

Type of Film	R_a	Film Thickness A°
Propionic Acid	11.9	3600 ± 175
Butyric Acid	9.8	2600 ± 150
Valeric Acid	8.2	1900 ± 75

Film thicknesses were measured as described in the experimental section. Films made with solutions at R_w=1.5 were used in this experiment.

R_a: molar ratio of acid to alkoxide
R_w: molar ratio of water to alkoxide

Table 4.7 Film thickness measurements of valeric acid films.

R_a	Film Thickness A°
6	2950 ± 75
8	2300 ± 40
10	1600 ± 60

Film thicknesses were measured as described in the experimental section. Films made with solutions at R_w=1.5 were used in this experiment.

R_a: molar ratio of acid to alkoxide
R_w: molar ratio of water to alkoxide

4.2 Encapsulation of the Metalloporphyrin Within the Porous Film

Dimerization and aggregation of free base porphyrins and their metal complexes are frequently encountered in solution, especially in aqueous media. Higher porphyrin concentrations promote aggregation. Generally, the blue shifted dimer Soret band shifts to longer wavelengths upon dilution [49, 50, 51]. In the absence of conflicting evidence, the presence of an isosbestic point in dilution studies suggests a monomer-dimer equilibrium in the system.

When films were made with solutions of the composition given in Table 3.1, but without the ethanol, the Soret band of the encapsulated PFPP shifted to the blue slowly, but continuously. The shift was from 410 nm to 350 nm. Figure 4.1 illustrates the observed spectral dynamics and Figure 4.2 illustrates the steady accumulation of the blue shifted peak.

Demetallation of PFPP is unlikely since strong acidic conditions are necessary to dislodge a metal from the porphyrin center. Any photo effect was discounted since PFPP in films stored in the dark followed the same trend. It was deemed unlikely that an alteration of the PFPP structure due to a reaction was taking place since controlled conditions are necessary to inflict changes to the thermodynamically stable porphyrin molecule (unless it reacts with strong donor ligands such as cyanide or carbon monoxide). Therefore, by the process of elimination, we attributed the instability demonstrated by spectral changes given in Figures 4.1 and 4.2 to aggregation of PFPP within the polymer matrix. Note that the spectral dynamics are consistent with that observed in the literature with aggregating systems.

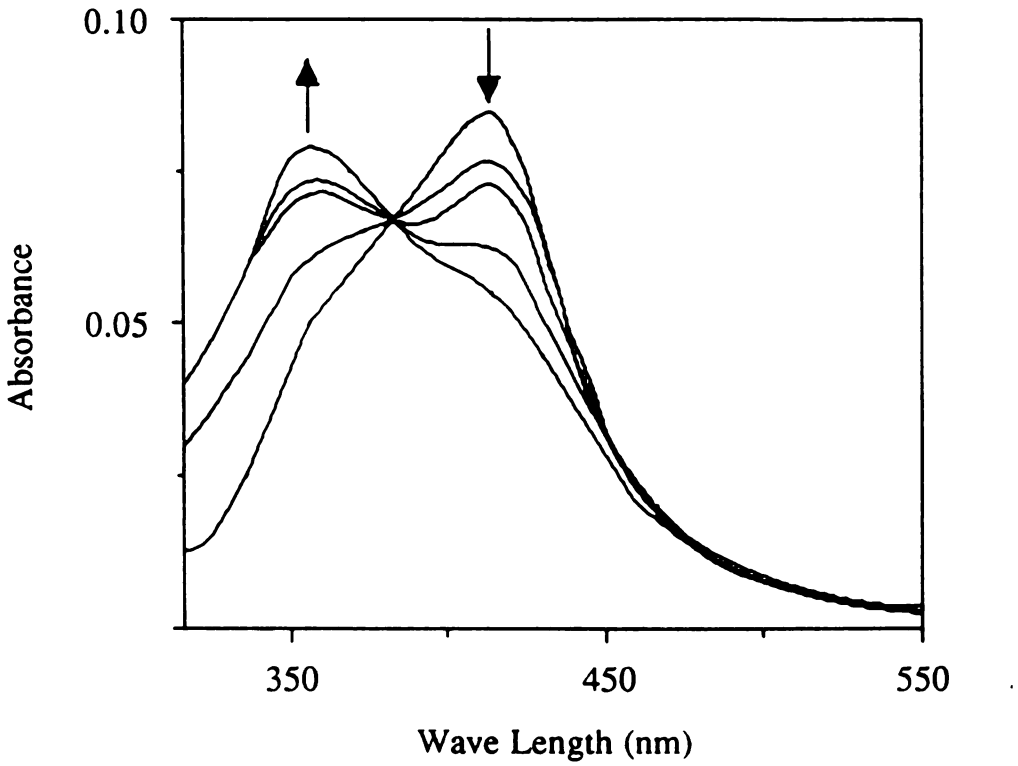

Figure 4.1 Spectral dynamics of PFPP entrapped in a valeric acid film. The film solution parameters were; R_a=9, R_w=1.5. The spectra were normalized to isolate the effect of aggregation from that of photodecomposition. The films were exposed to room light and ambient conditions during the period these changes were observed.

R_a = molar ratio of acid to alkoxide
R_w = molar ratio of water to alkoxide

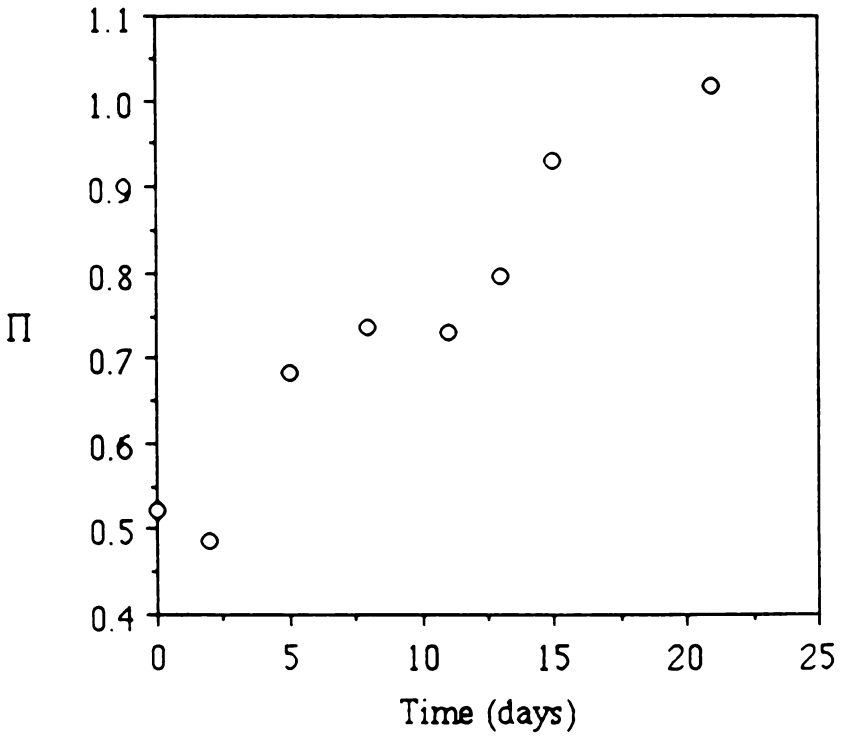

Figure 4.2 Plot of Π vs. Time. Data from Figure 4.1.

$$\Pi = \frac{\text{Absorbance at 350 nm}}{\text{Absorbance at 410 nm}}$$

Sol-gel material by classification are fluids. Therefore, we speculated that the fluidity of the film structure may allow the porphyrin molecules to be mobile thus promoting aggregation. Further, it is possible that the polymer matrix may not have reached thermodynamic equilibrium in terms of matrix formation and thus a dynamic structure. Long equilibration times for matrix formation in sol-gel systems is not surprising due to the complexity of the reaction dynamics.

Stabilization of the matrix was of primary importance to the implementation of a successful sensor system since preliminary investigations proved that overly aggregated systems are not responsive to cyanide ions. Experimentation with modification techniques available in the sol-gel process was the logical next step toward matrix stabilization. One such technique was alcoholysis. Its traits were discussed in Section 2.1.4.

The reviewed porphyrin literature revealed that ethanol was capable of dispersing porphyrin aggregates in solution [51, 55]. Lowering of the dielectric constant of the solution upon the addition of ethanol is responsible for this effect. Ethanol, in addition to being a dispersive agent, can participate in alcoholysis in sol-gel systems. Consequently, the two fold effectiveness of ethanol rendered it the candidacy for initial stabilization experiments.

Even though aggregation of PFPP in the film solution was not observed experimentally due to instrumental limitations, it is reasonable to suppose that it originates in the film solution. The high porphyrin concentration, approximately 2×10^{-3} M, is likely to initiate such an event.

It is also likely that the control of aggregation in the film solution transcends to the film phase.

Ethanol was added to the film solution containing PFPP soon after the addition of water. The film composition was given in Table 3.1. The effect of varied amounts of ethanol on the system is presented in Table 4.8.

Porphyrins and metalloporphyrins are known to decompose upon exposure to light. Photodecomposition of encapsulated PFPP was observed in preliminary experiments. However, the results presented in Table 4.8 indicate that, modifications to the sol-gel system initiated by ethanol contribute to the partial control of the rate of photodecomposition of encapsulated PFPP. One milliliter of added ethanol is accompanied by a 70 % loss in absorbance intensity over a period of 42 days. In contrast, only a 15 % reduction was observed when 4 ml of ethanol was used. It is possible that an alteration to the extent or the nature of electronic interaction between the porphyrin and the titanium based polymer matrix may have contributed to this stabilization effect. It may also be possible that the new material is capable of acting as a "light-sink" at critical wave lengths that decompose the porphyrin.

The comparison of the initial (1^{st} day) absorbance measurements of the films prepared with 1 ml ethanol and 4 ml ethanol gives nearly a six fold intensity enhancement in favor of the latter condition. The phenomenon resembles an instant where the suppressed electronic transitions have been refurbished. The exact cause for such a rejuvenation is yet unclear. Again the most likely explanation would be a favorable alteration of the guest-host electronic interactions.

Table 4.8 The effect of ethanol on the photodecomposition of entrapped PFPP.

Sample Number *	Absorbance at 410 nm **				Total % Loss ***
	1st day	7th day	21st day	42nd day	
1	0.057	0.026	0.026	0.017	70.2
2	0.097	0.065	0.055	0.042	56.7
3	0.214	0.220	-	0.160	25.2
4	0.332	0.332	0.300	0.280	15.7

* 1 = 1 ml of ethanol
2 = 2 ml of ethanol
3 = 3 ml of ethanol
4 = 4 ml of ethanol

** The day on which the absorbance of the encapculated PFPP was observed counting from the day the films were cast

*** The percent loss in absorbance intensity calculated after 42 days. The entrapped PFPP was exposed to room light and ambient conditions.

The primary objective of this segment of the project was to study the possibility of controlling aggregation of encapsulated PFPP. The absorbance of PFPP encapsulated in films made from solutions of the composition given in Table 4.9 were monitored for a period exceeding one month. Over the span of this experiment some films were stored in a dark environment and some were exposed to room light in order to avoid ambiguities that may arise from untested photo effects. None showed any sign of aggregation; that is, the growth of the band of PFPP at 350 nm was completely curtailed in films modified by ethanol. It is clear that the modified chemical composition of the film solution has been effective in transfiguring the polymer matrix to a less fluid host. Consequently, PFPP is held in place as monomers. Presumably, PFPP exists as dispersed monomers in film solutions containing ethanol, since ethanol is effective in dispersing aggregates. In turn, this would help give a more dispersed porphyrin distribution in the film, further deterring the aggregation process.

Table 4.9 Composition of the modified PFPP incorporated film solution.

Component	Molar Ratio (R^*)
PFPP	$R_p = 0.008$
Valeric Acid	$R_a = 9.0$
Water	$R_w = 1.5$
Ethanol	$R_e = 40^{**}$

* molar ratio with respect to the alkoxide
** equivalent to the composition of Sample 4 in Table 4.8

The realized stability of the guest-host system proved that the modification technique adopted was a judicious choice. Even though, the

exact course through which ethanol executed the stabilization process is yet unknown, it is reasonable to suppose that both dispersion of aggregates and structural modification, in combination, was able to enforce stability to the system. Alcoholysis of the propoxy groups of the titanium alkoxide by ethoxide groups potentially changes the reactivity of the alkoxide; consequently, hydrolysis and polycondensation is affected. The compounded outcome is an alteration to the polymer configuration. In addition, since ethanol is used in excess, the dilution of the reacting species in ethanol may change reaction kinetics and thermodynamics significantly, giving an alternative equilibrium composition. A detailed characterization is beyond the scope of this project.

The usable life time of the film solution is approximately three weeks. Films made with solutions aged over four weeks exhibit increasingly poorer adhesion properties. The relative stability of the film solutions over a period of three weeks is likely due to substituted carboxylic acid groups acting as terminators of polycondensation reactions that lead to gel formation. The activity that instigates poor adhesion properties of films made with solutions aged over four weeks is not clear. However, it is possible that due to the presence of an excess amount of carboxylic acid groups, the polymer structure is broken down at the titanium metal by further acid substitution. This could lead to discontinuity in the polymer structure and also more hydrophobicity, thus resulting in poor adhesion.

4.3 The Cyanide Sensor

4.3.1 Making of the Cyanide Sensor

In order to determine the appropriate parameters for the sensor calibration, films were treated with a 400 ppm cyanide solution. Spectral changes were recorded at steady time increments. Spectra recorded over a period of 15 min. are given in Figure 4.3. The Soret absorbance maximum of encapsulated PFPP is at 410 nm. Upon the introduction of aqueous cyanide, the Soret absorbance maximum red shifts to 430 nm. The isosbestic point verifies the presence of two absorbing species; presumably, the second being the cyanide complexed PFPP. At this point, it is not possible to comment on the nature of the complexation, i.e. the value of n (see Section 2.2.5), since data analysis of heterogeneous reaction kinetics coupled to resistance to mass transport is necessary for a reasonable conclusion.

When films containing PFPP were soaked in water, no detectable amounts of PFPP was observed to leach to the solution. However, upon complexation with cyanide, trace amounts of complexed PFPP was detected in the aqueous cyanide solution. At 25,000 ppm cyanide ion concentration, the percent leached to the solution was approximately 5 % with respect to the total absorbance measured at 430 nm. Leaching was not detectable at low cyanide ion concentrations. Even though the leached porphyrin was quantitatively significant at high cyanide ion concentrations, the leaching was not considered to be restrictive toward a reasonable calibration.

Figure 4.3 suggests that the obvious choice for an internally standardized calibration parameter for the sensor would be the ratio absorbance at 430 nm to absorbance at 410 nm. The choice of a ratio

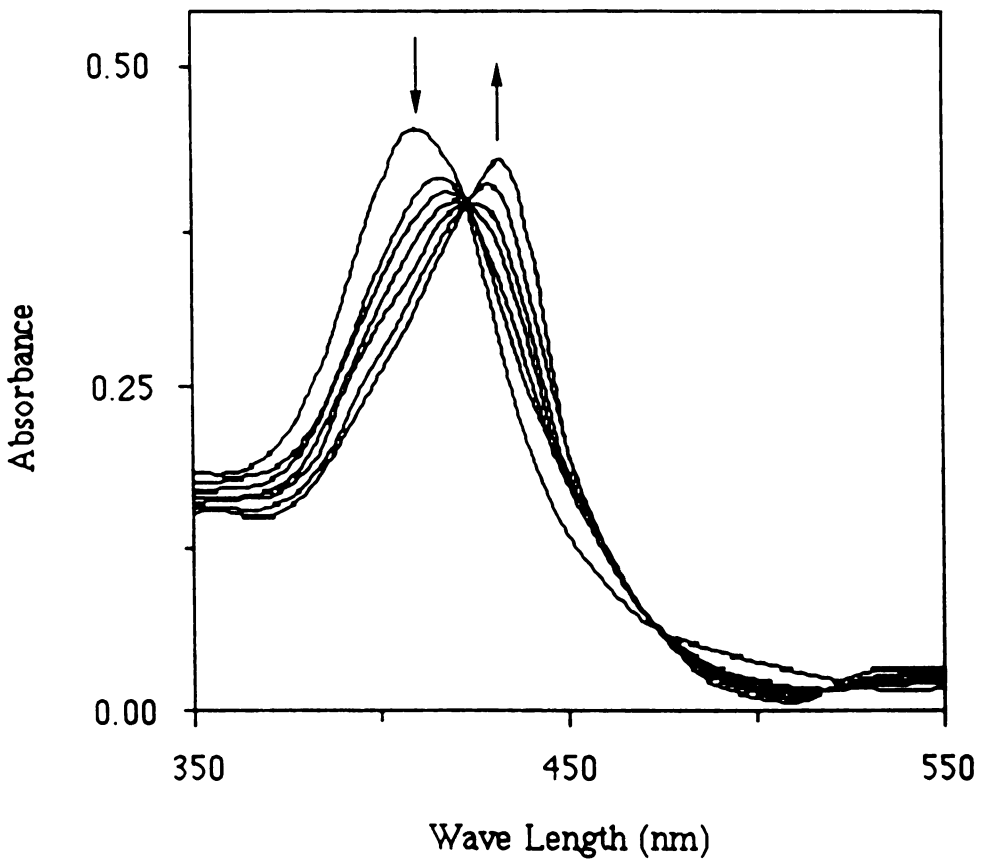

Figure 4.3 Spectral dynamics of PFPP entrapped in a valeric acid film upon contacting the film surface with an aqueous cyanide solution. Film solution parameters are as follows; R_a=9, R_w=1.5, R_e=40, R_p=0.008. Spectra were recorded for 15 min. The initial bulk cyanide ion concentration was 400 ppm.

R_a = molar ratio of acid to alkoxide
R_w = molar ratio of water to alkoxide
R_e = molar ratio of ethanol to alkoxide
R_p = molar ratio of PFPP to alkoxide

reflecting the relative amounts of both product and reactant as the calibration parameter is particularly advisable since it will not be affected by instrumental drift. In the proceeding discussion the calibration parameter will be identified by the symbol Ø. The plot of Ø vs. time is given in Figure 4.4. A 15 min. sensor response time seemed to be adequate.

Spectra of film-encapsulated PFPP and that of PFPP dissolved in a solution comprised of 10 % (V/V) water in ethanol were similar in appearance. The response of PFPP to cyanide ions, in both situations, was also similar (compare spectral dynamics of Figure 4.3 to that of Figure 4.5). The similarity of the PFPP spectra and spectral dynamics in solution and in the heterogeneous polymeric environment indicates that the major characteristics of PFPP has been retained. The time scale of the response in solution was less than one second compared to 15 min. required in the film. Mass transport considerations are most likely responsible for the sluggishness of the sensor response.

4.3.2 The Sensor

Figures 4.6 and 4.7 show the detectable range of the sensor. The lower limit is approximately 40 ppm (see Figure 4.6) and the upper limit is approximately 25,000 ppm (see Figure 4.7). Below 40 ppm the changes in CN^- ion concentration does not provoke significant changes to Ø. At 25,000 ppm, Ø reaches an asymptote, suggesting that the encapsulated PFPP available for complexation is being effectively saturated.

A linear calibration for the sensor was obtained by plotting Ø, measured after 15 min. of treatment, vs. the logarithm of the CN^- ion concentration. The linear calibration is given in Figure 4.8. The plotted

data represents analysis of six different sets of films at each given concentration. In addition, the films used for analysis were aged between three and thirty days. The calibration indicates that the sensor has a large dynamic range for the detection of CN^- ions. The sensor is stable and functional over a period of one month (stability beyond one month has to be tested), suggesting that the approach can be applied to manufacturing sensors with long shelf lives.

The work presented herein, has clearly demonstrated the viability of integrating sol-gel polymer matrices and relevant chemistries to construct sensor devices. The method is particularly advantageous for analytes for which there are no direct indicators.

The inability of this particular sensor system to respond at lower analyte concentrations is not surprising. The chemical behavior of the probe encapsulated in a microheterogeneous medium can be quite different from that observed in a homogeneous environment. A number of factors may affect the sensitivity of the probe. Some of the eminent contributory factors are examined below.

Probe Rigidity: When probe molecules are encapsulated in a microheterogeneous environment such as the metallo-organic polymer matrix utilized here, the mobility of the probe can be restricted to pockets or cages circumvented by polymer material or even to restricted dimensions. Conditions for chemical reaction in such a system are in sharp contrast to that afforded by simple homogeneous systems. The resulting anisotropic molecular motions are bound to adversely affect the kinetics and thermodynamics of the probe-analyte reaction. A diminished response is the final outcome.

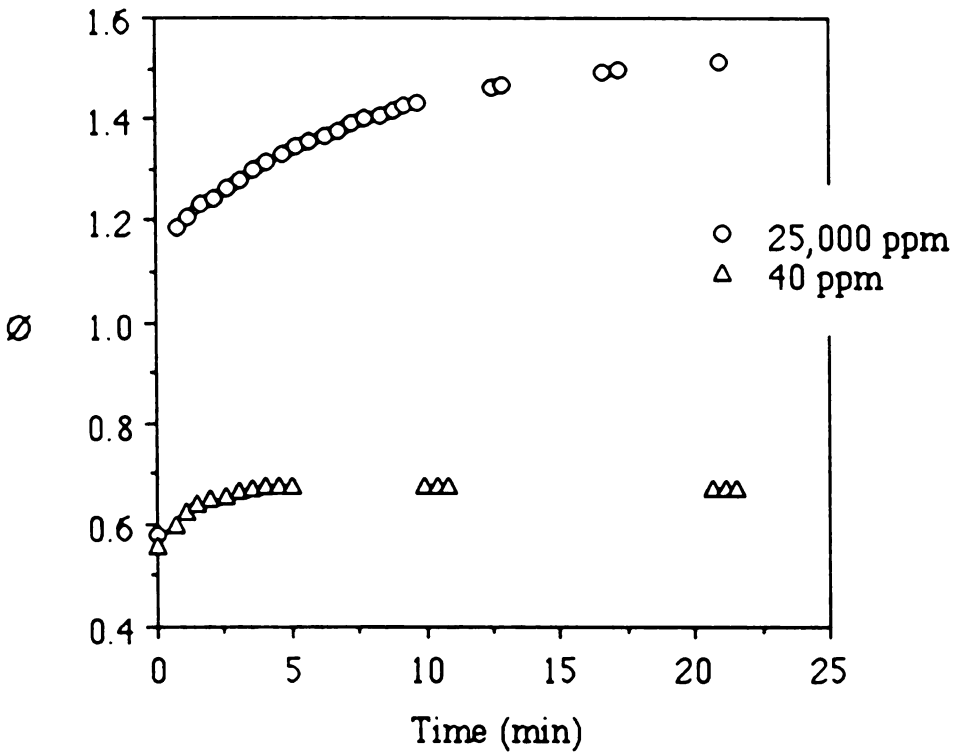

Figure 4.4 Plot of Ø vs. Time at cyanide ion concentrations of 40 ppm (low) and 25,000 ppm (high).

$$Ø = \frac{\text{absorbance at 430 nm}}{\text{absorbance at 410 nm}}$$

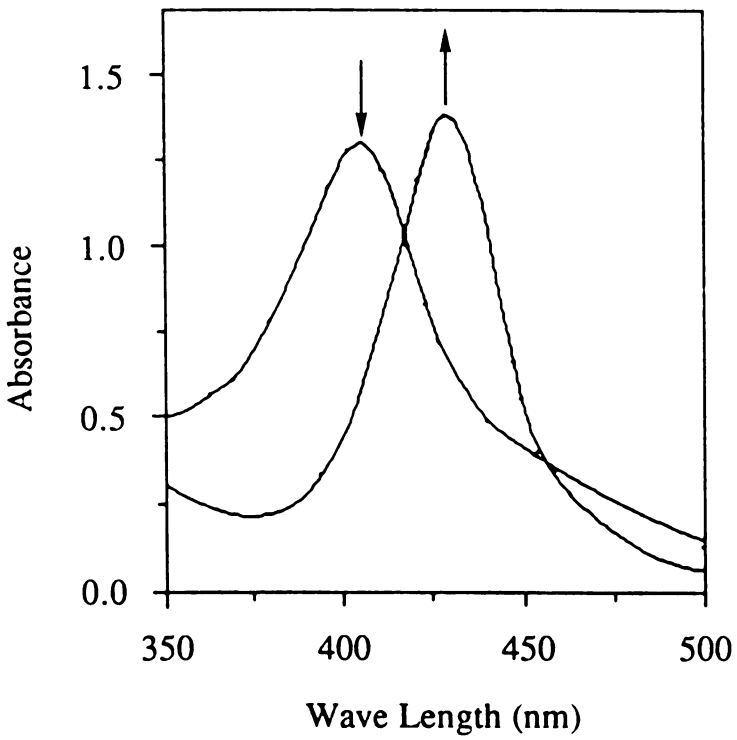

Figure 4.5 Spectral dynamics of PFPP upon reacting with cyanide in a 10% (V/V) water, 90% (V/V) ethanol mixture. Approximate concentrations were; [PFPP]=20 ppm and [CN^-]=400 ppm. The spectra were obtained by adding cyanide dissolved in water to PFPP contained in ethanol. The spectral transformations indicated by the arrows (the growth of the peak near 430 nm and the disappearence of the peak near 410 nm) took place within 6 seconds.

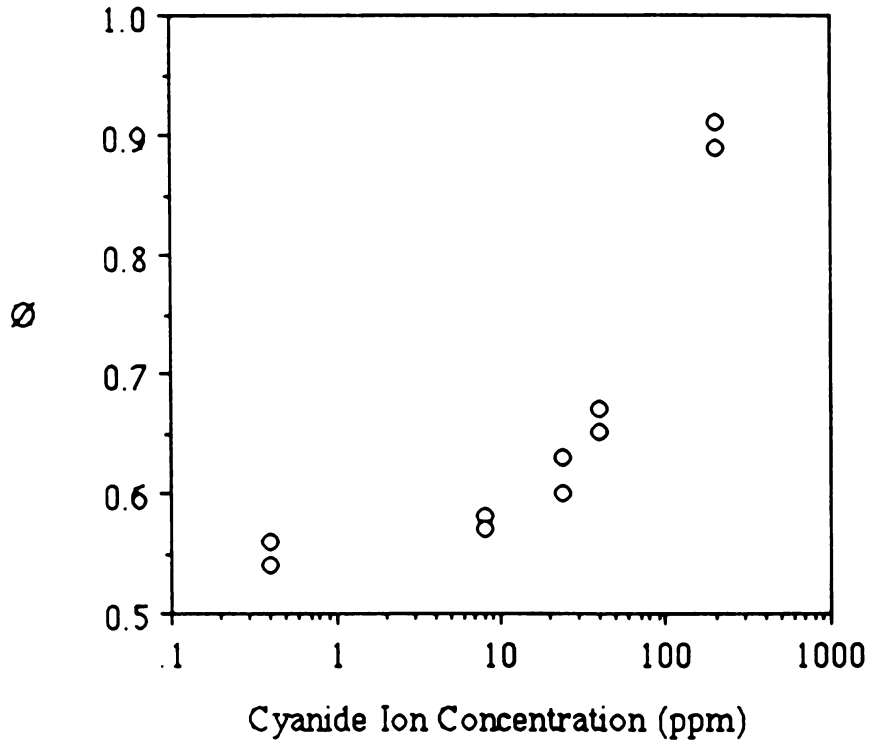

Figure 4.6 Plot of Ø vs. cyanide ion concentration near the lower bound of the detector range. The parameter Ø was measured 15 min. after treatment.

$$\text{Ø} = \frac{\text{absorbance at 430 nm}}{\text{absorbance at 410 nm}}$$

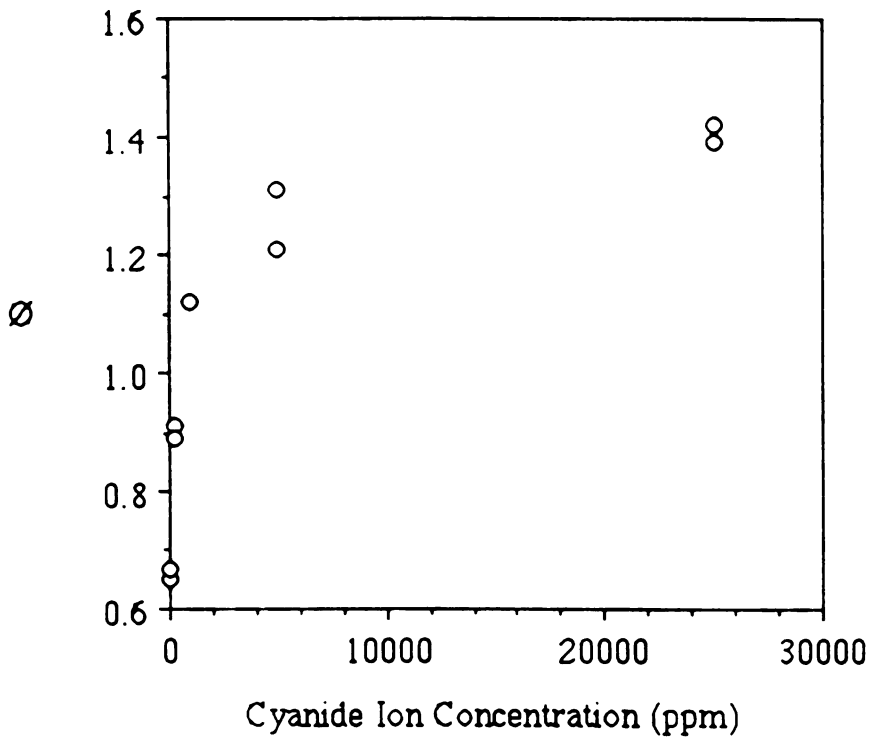

Figure 4.7 Plot of Ø vs. cyanide ion concentration showing the upper bound of the detector range. The parameter Ø was measured 15 min. after treatment.

$$\text{Ø} = \frac{\text{absorbance at 430 nm}}{\text{absorbance at 410 nm}}$$

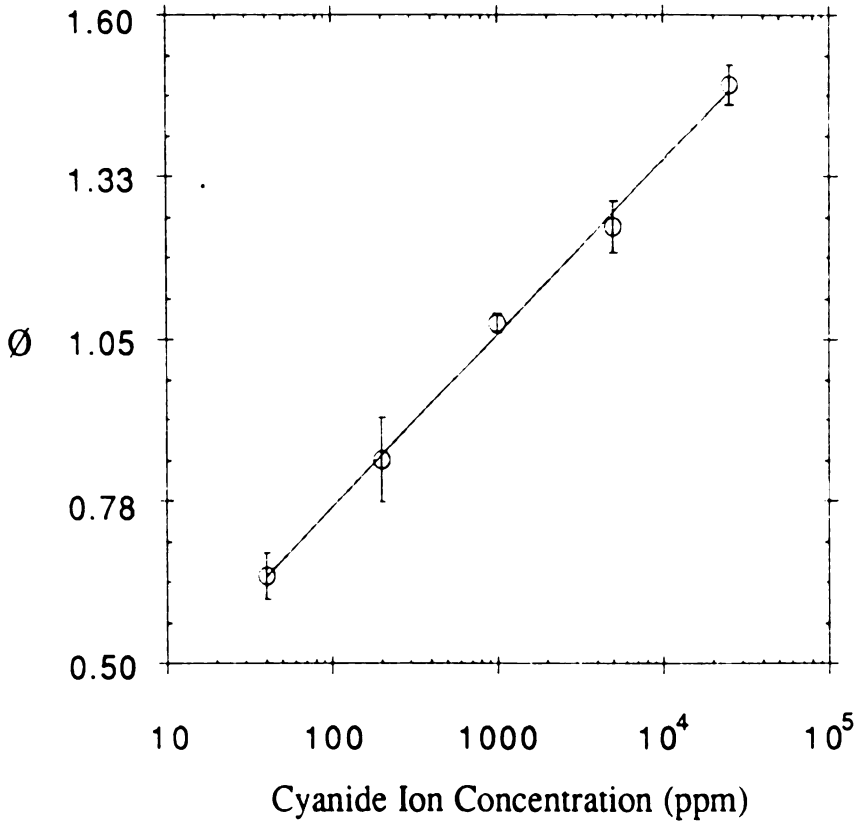

Figure 4.8 The sensor calibration. The parameter Ø was measured 15 min. after treatment.

$$\text{Ø} = \frac{\text{absorbance at 430 nm}}{\text{absorbance at 410nm}}$$

Conformational Restraints: In microheterogeneous systems, conformational restraints of the probe are consequences of hindered molecular mobility imposed by the system. Probe molecules may be forced to assume anomalous orientations or conformations atypical of those encountered in homogeneous media. Skewed geometries of probe molecules can influence the efficiency of reaction with relevant analytes thereby drastically decreasing the sensor response.

Presence of Local Electric Fields: A common attribute of most organized assemblies is the presence of local electric fields arising from systematized charge distributions. Electrostatic static forces so incumbent in the host system can distort the charge distribution of the probe molecule and in turn alter its chemical characteristics.

The system possesses some flexibility to adjust the range of analyte concentration within which the sensor is responsive. For instance a higher concentration of PFPP within the polymer matrix may have responded to lower concentrations of cyanide. However, using higher concentrations of porphyrins may be counterproductive since they tend to aggregate more readily at higher concentrations. The remarkable success in controlling aggregation accomplished in this work, in part through structural modifications initiated by alcoholysis, suggests that overcoming aggregation at higher concentrations would not be an insurmountable task. It is also possible to select a probe molecule that is inherently stable.

The work reviewed in Section 2.2.2 indicates that the kinetics and thermodynamics of anation reactions are affected by, among other things, the nature of the porphyrin macrocycle and the peripheral groups. Therefore, an alternative to using higher concentrations of metalloporphyrins is to investigate the possibility of using a porphyrin

macrocycle that would favor a higher extent of complexation at the same conditions. For example, a weak donor porphyrin macrocycle would promote axial binding of donor ligands. However, it would have limited capability to stabilize the axial bond through backbonding and therefore would not lead to higher extents of reaction. In contrast, a porphyrin macrocycle that has the ability to donate electrons to the empty π-orbitals of the donor ligand would strengthen the axial bond resulting in a higher extent of complexation. Therefore, the utilization of an alternate metalloporphyrin possessing favorable thermodynamic properties may lead to the development of a cyanide sensor with a better response.

The ideal sensing system would be one that is reversible and reusable. The system developed here lacks this quality since extreme conditions are necessary to dislodge the cyanide from the metal. Such conditions are bound to be detrimental to the stability of sol-gel derived polymer matrices. For example, the films developed in this work are stable only in the narrow pH range of 4 to 7. However, readily reversible chemistries involving other analytes and probe molecules would not be effected. A pragmatic solution that avoids problems encountered in the development of reversible and reusable sensors is the construction of inexpensive, single use and disposable / recyclable test kits. Sol-gel material and the process is well suited for the manufacture of economically viable and environmentally friendly polymer matrix supports.

The results of this work conforms the possibility of fabricating dry-chemistry sensory devices using sol-gel derived thin films where all necessary reagents are contained in dry form in a disposable test strip. This method allows an untrained person to measure the concentration of a substance using a standard calibration. Such devises can be used to analyze

streams of pharmaceutical processes, agricultural and industrial waste effecting the environment and can also be used in human and animal diagnosis.

In addition to the simplicity and the operational ease common to dry-chemistry techniques, the sol-gel method used to make the structure of the sensor in this model system makes such systems very cost effective. Ambient conditions and small amounts of precursors are used. Mass production of these sensor strips can be easily accomplished and packaging poses no difficulty. Inexpensive hand held spectrophotometers are available for quick analysis when needed.

5 Conclusions

The routine sol-gel process can be successfully modified to produce thin films. Control of hydrolysis has a profound effect on the production of films. The judicious choice of modifying reagents lead to quality films having productive properties such as optical transparency, high porosity, thermal and mechanical stability, resistance to aqueous and organic solvents, excellent adhesion and uniformity.

Probe molecules having good solubility properties can be encapsulated within the polymer matrix such that they are accessible to reactive exogenous species. The metalloporphyrin-cyanide ion combination used here serves as an example for other probe-analyte systems. The control of aggregation of PFPP by ethanol induced alcoholysis on modified titanium alkoxides, manifests the versatility of the modification techniques available in the sol-gel process toward making functional sensor systems.

The success of this work indicates that spectroscopic changes incurred by probe molecules encapsulated in sol-gel derived films can be conveniently calibrated to quantify unknown amounts of analyte. Generality of the approach is thus clear.

Appendix

6 Appendix: Raw Data Used in the Preparation of Figures

Table A.1 Data for Figure 4.2.

Time (Days)	Absorbance at 410 nm	Absorbance at 350 nm	Π
0	0.096	0.050	0.521
2	0.078	0.038	0.487
5	0.066	0.045	0.682
8	0.068	0.050	0.735
11	0.063	0.046	0.730
13	0.059	0.047	0.797
15	0.057	0.053	0.930
21	0.060	0.061	1.017

$$\Pi = \frac{\text{absorbance at 430 nm}}{\text{absorbance at 410 nm}}$$

Table A.2 Data for Figure 4.4.

a. At 25,000 ppm, initial bulk cyanide concentration

Time (min)	Absorbance at 430 nm	Absorbance at 410 nm	Ø
0.00	0.212	0.367	0.578
0.83	0.340	0.287	1.185
1.20	0.343	0.284	1.208
1.70	0.346	0.281	1.231
2.13	0.348	0.280	1.243
2.63	0.351	0.278	1.263
3.12	0.353	0.276	1.279
3.63	0.354	0.273	1.297
4.13	0.355	0.270	1.315
4.68	0.356	0.268	1.328
5.20	0.358	0.266	1.346
5.73	0.359	0.265	1.355
6.27	0.360	0.264	1.364
6.77	0.362	0.263	1.376
7.28	0.363	0.261	1.391
7.78	0.364	0.260	1.400
8.33	0.364	0.259	1.405
8.85	0.366	0.258	1.419
9.28	0.366	0.257	1.424
9.73	0.366	0.256	1.430
12.47	0.368	0.252	1.460
12.92	0.368	0.251	1.466
16.62	0.370	0.248	1.492
17.18	0.370	0.247	1.498
20.97	0.372	0.246	1.512

$$\text{Ø} = \frac{\text{absorbance at 430 nm}}{\text{absorbance at 410 nm}}$$

Table A.2 cont'n

b. At 40 ppm, initial bulk cyanide concentration

Time (min)	Absorbance at 430 nm	Absorbance at 410 nm	Ø
0.00	0.205	0.366	0.560
0.68	0.215	0.358	0.601
1.12	0.220	0.352	0.625
1.52	0.222	0.348	0.638
1.98	0.225	0.345	0.652
2.53	0.226	0.344	0.657
3.02	0.227	0.342	0.664
3.57	0.228	0.341	0.669
4.07	0.229	0.340	0.674
4.53	0.229	0.339	0.676
4.98	0.229	0.339	0.676
9.93	0.229	0.338	0.678
10.42	0.229	0.338	0.678
10.85	0.229	0.338	0.678
20.72	0.227	0.339	0.670
21.12	0.227	0.339	0.670
21.60	0.227	0.339	0.670

$$\text{Ø} = \frac{\text{absorbance at 430 nm}}{\text{absorbance at 410 nm}}$$

Table A.3 Data for Figures 4.6 and 4.7.

[Cyanide] ppm	Absorbance at 430 nm	Absorbance at 410 nm	Ø
0.4	0.161	0.289	0.56
0.4	0.176	0.327	0.54
8	0.207	0.359	0.58
8	0.183	0.323	0.57
24	0.220	0.349	0.63
24	0.212	0.352	0.60
40	0.229	0.353	0.65
40	0.236	0.352	0.67
200	0.272	0.300	0.91
200	0.254	0.285	0.89
1000	0.292	0.260	1.12
1000	0.291	0.259	1.12
5000	0.338	0.259	1.31
5000	0.308	0.254	1.21
25000	0.355	0.250	1.42
25000	0.358	0.258	1.39

$$\text{Ø} = \frac{\text{absorbance at 430 nm}}{\text{absorbance at 410 nm}}$$

Table A.4 Data for Figure 4.8.

Films aged for 3 days

[cyanide] (ppm)	Absorbance at 430 nm	absorbance at 410 nm	Ø
25000	0.364	0.236	1.54
25000	0.370	0.248	1.49
5000	0.346	0.269	1.29
5000	0.343	0.272	1.26
1000	0.271	0.348	0.78
1000	0.301	0.281	1.07
200	0.275	0.312	0.88
200	0.261	0.294	0.89
40	0.228	0.338	0.67
40	0.244	0.349	0.70

Films aged for 15 days

[cyanide] (ppm)	Absorbance at 430 nm	absorbance at 410 nm	Ø
25000	0.410	0.284	1.44
25000	0.442	0.302	1.46
5000	0.373	0.295	1.26
5000	0.379	0.300	1.26
1000	0.352	0.323	1.09
1000	0.334	0.303	1.10
200	0.320	0.347	0.92
200	0.295	0.338	0.87
40	0.267	0.404	0.66
40	0.267	0.412	0.65

$$\text{Ø} = \frac{\text{absorbance at 430 nm}}{\text{absorbance at 410 nm}}$$

Table A.4 Cont'n.

Films aged for 30 days

[cyanide] (ppm)	Absorbance at 430 nm	Absorbance at 410 nm	Ø
25000	0.363	0.246	1.48
25000	0.366	0.248	1.48
5000	0.370	0.310	1.19
5000	0.376	0.319	1.18
1000	0.324	0.304	1.07
1000	0.316	0.298	1.06
200	0.255	0.336	0.76
200	0.270	0.358	0.75
40	0.220	0.372	0.59
40	0.249	0.403	0.62

$$\text{Ø} = \frac{\text{absorbance at 430 nm}}{\text{absorbance at 410 nm}}$$

List of References

7 List of References

1. M. Ebelmen, *Ann. Chim Phys.*, **16**, (1946), 129.

2. H. Reuter, *Adv. Mater.*, **3:5**, (1991), 258.

3. J. Livage, M. Henry and C. Sanchez, *Progress in Solid State Chemistry*, **18**, (1988), 259.

4. H. Zheng, M. W. Colby and J. D. Mackenzie in: Better Ceramics Through Chemistry III, C. J. Brinker, D. E. Clark and D. R. Ulrichs, Eds., (Materials Research Society, Reno, Nevada, U.S.A., 1988), vol. 121, p. 537.

5. M. Prassas and L. L. Hench, Ultrastructure Processing of Ceramics: Glasses and Composites (Wiley, New York, 1984), p.100.

6. W. C. Lacourse and S. Kim, Science of Ceramic Processing (Wiley, New York, 1986), ch.305-310.

7. K. Kamiya et al., *JMSL*, **5**, (1986), 402.

8. J. Philipp and H. Schmidt, *J. Non-Cryst. Solids*, **82**, (1986), 31.

9. M. Guglielmi and G. Carturan, *J. Non-Cryst. Solids*, **100**, (1988), 16.

10. R. L. Martin and G. Winter, *J. Chem. Soc.*, (1961), 2947.

11. D. C. Bradley, R. Gaze and W. Wardlaw, *J. Chem. Soc.*, (1955), 3977.

12. a. T. Boyd, *J. Polym. Sci.*, **7**, (1951), 591.
    b. D. C. Bradley, R. Gaze and W. Wardlaw, *J. Chem. Soc.*, (1955), 721.
    c. S. Minami and T. Ishino, *Technol. Rept. Osaka Univ.*, **3**, (1953), 357.
    d. D. C. Bradley, R. Gaze and W. Wardlaw, *J. Chem. Soc.*, (1957), 469.

e. K. A. Berglund, D. R. Tallant and R. G. Dosch, in: Science of Ceramic Chemical Processing, L. L. Hench and D. R. Ulrich, Eds., (John Wiley & Sons, New York, 1986), p. 94.

13. D. C. Bradley, R. C. Mehrotra and D. P. Gaur, Metal Alkoxides (Academic Press, New York, 1978).

14. K. Kamiya, K. Tanimoto and T. Yoko, *J. Mat. Sci. Lett.*, **5**, (1986), 402.

15. U. S. Patent 3,640,093, (assigned to L. Levene and I. M. Thomas), 1972.

16. M. Yamane, S. Inoue and K. Nakazawa, *J. Non-Cryst. Solids*, (1982), 153.

17. A. E. Martell, Advances in Chemistry Series (American Chemical Society, Washington D.C., 1967), No. 62.

18. C. Guizard, N. Cygankiewicz, A. Larbot and L. Cot, *J. Non-Cryst. Solids*, **82**, (1986), 86.

19. S. Doeuff, M. Henry, C. Sanchez and J. Livage, *J. Non-Cryst. Solids*, **89**, (1987), 84.

20. S. Doueff, M. Henry, C. Sanchez and J. Livage, *J. Non-Cryst. Solids*, **89**, (1987), 206.

21. C. Sanchez, F. Babonneau, S. doeuff and A. Leaustic, in: Ultrastructure Processing of Ceramics Glasses and Composites, J. D. Mackenzie and D. R. Ulrichs, Eds., (San Diego, CA, U.S.A., 1986 Feb.).

22. F. Basolo and R. G. Pearson, Mechanisms of Inorganic Reactions (J. Wiley & Sons, New York, 1967, 2nd Edition).

23. T. Woignier, J. Phalippou and J. Zarzycki, *J. Non-Cryst. Solids*, **63**, (1984), 117.

24. I. D. Verma and R. C. Mehrotra, *J. Chem. Soc.*, (1960), 2966.

25. H. Schmidt, G. Rinn, R. Nab and D. Sporn, in: Better Ceramics Through Chemistry III, C. J. Brinker, D. E. Clark and D. R. Ulrichs, Eds., (Materials Research Society, Reno, Nevada, U.S.A., 1988), vol. 121, p. 743.

26. S. M. Melpolder and B. K. Coltrain, in: Better Ceramics Through Chemistry III, C. J. Brinker, D. E. Clark and D. R. Ulrichs, Eds., (Materials Research Society, Reno, Nevada, U.S.A., 1988), vol. 121, p. 811.

27. L. F. Thompson and M. J. Bowden, in: Introduction to Microlithography, L. F. Thompson, C. G. Willson and M. J. Bowden, Eds., (American Chemical Society Symposium 219, Seattle, WA, U.S.A., 1983) ch. 161.

28. R. Bonnett, in: The Porphyrins: Structure and Synthesis, Part A, D. Dolphin, Ed. (Academic Press, New York, 1978), vol. 1, ch. 9.

29. J. W. Buchler, in: The Porphyrins: Structure and Synthesis, Part A, D. Dolphin, Ed. (Academic Press, New York, 1978), vol. 1, ch. 10.

30. J. E. Falk, Porphyrins and Metalloporphyrins, (Elsevier Publishing Company, New York, 1964), vol. 2, ch. 3.

31. P. Hambright and P. B. Chock, *J. inorg. nucl. Chem.*, **37**, (1975), 2363.

32. a. L. Stryer, J. C. Kendrew and H. C. Watson, *J. Mol. Biol.*, **8**, (1964), 96.
    b. C. L. Nobbs, H. C. Watson, and J. C. Kendrew, *Nature (London)*, **209**, (1966), 339.
    c. H. Muirhead, and J. Green, *Nature (London)*, **228**, (1970), 516.

33. E. H. Abbott and P. A. Rafson, *J. Am. Chem. Soc.*, **96:23**, (1974), 7378.

34. M. A. Stanford, J. C. Swartz, T. E. Phillips and B. M. Hoffman, *J. Am. Chem. Soc.*, **102:13**, (1980), 4492.

35. a. S. Modi, V. P. Shedbalkar and D. V. Behere, *Inorganica Chimica Acta*, **173**, (1990), 9.
b. G. J. Del and G. N. La Mar, *J. Am. Chem. Soc.*, **98**, (1976), 3014.

36. G. N. La. Mar and J. D. Gaudio, *Adv. Chem. Ser., Bioinorg. Chem. II Symp.*, **162**, (1977), 207.

37. L. M. Epstein, D. K. Straub and C. Maricondi, *Inorg. Chem.*, **6**, (1967), 1720.

38. J. D. Gaudio and G. N. La. Mar, *J. Am. Chem. Soc.*, **98:10**, (1976), Communications to the Editor.

39. K. M. Kadish, M. M. Morrison, L. A. Constant and L. Dickens, *J. Am. Chem. Soc.*, **98**, (1976), 8387.

40. a. M. G. Reinecke, J. H W Johnson and J. F. Sebastian, *J. Am. Chem. Soc.*, **91**, (1969), 3817.
b. S. J. Cole, G. C. Curthoys and E. A. Magnusson, *J. Am. Chem. Soc.*, **93:9**, (1971), 2153.

41. J. E. Falk, Porphyrins and Metalloporphyrins (Elsevier Publishing Company, New York, 1964), vol. 2, ch. 6.

42. a. W. M. Clark and M. E. Perkins, *J. Biol. Chem.*, **135**, (1940), 643.
b. R. W. Cowgill and W. M. Clark, *J. Biol. Chem.*, **198**, (1952), 33.

43. H. Fischer and H. Bock, *Z. Physiol. Chem.*, **255**, (1938), 1.

44. a. Q. H. Gibson and S. Ainsworth, *Nature (London)*, **180**, (1957), 1416.
b. D. Mauzerall, *J. Am. Chem. Soc.*, **82**, (1960), 1832.
c. G. R. Seely and M. Calvin, *J. Chem. Phys.*, **23**, (1955), 1068.

45. a. W. M. Dale and C. Russell, *Biochem. J.*, **62**, (1956), 50.
b. H. B. Hamilton, S. Okada and M. Morrison, *Biochim. Biophys. Acta*, **23**, (1957), 540.
c. H. Laser, *Nature (London)*, **176**, (1955), 361.
d. M. L. Rothschild, L. Cosi and J. L S Myers, *Nature (London)*, **182**, (1958), 316.

46. A. E. Alexander, *J. Chem. Soc.*, (1937), 1813.

47. J. A. Bergeron, J. G L Gaines and W. D. Bellamy, *J. Colloid Interface Sci.*, **25**, (1967), 97.

48. W. I. White, in: The Porphyrins: Physical Chemistry, Part C, D. Dolphin, Ed., (Academic Press, New York, 1978), vol. V, ch. 7.

49. R. F. Pasternack, L. Francesconi, D. Raff and E. Spiro, *Inorg. Chem.*, **12:11**, (1973), 2606.

50. J. A. Shelnutt, M. M. Dobry and J. D. Satterlee, *J. Phys. Chem.*, **88**, (1984), 4980.

51. W. I. White and R. A. Plane, *Bioinorg. Chem.*, **4**, (1974), 21.

52. a. R. F. Pasternack, et al., *J. Am. Chem. Soc.*, **94**, (1972), 4511.
    b. R. R. Das, R. F. Pasternack and R. A. Plane, *J. Am. Chem. Soc.*, **92**, (1970), 3312.
    c. J. H. Fuhrhop, P. Wasser, D. Riesner and D. Mauzerall, *J. Am. Chem. Soc.*, **94**, (1972), 7996.

53. R. J. Kassner and J. H. Wang, *J. Am. Chem. Soc.*, **88**, (1966), 5170.

54. W. A. Gallagher and W. B. Elliott, *Ann. N.Y. Acad. Sci.*, **206**, (1973), 463.

55. a. M. H. Smith, *Biochem. J.*, **73**, (1959), 90.
    b. W. A. Gallagher and W. B. Elliott, *Biochem. J.*, **97**, (1965), 187.
    c. J. Shack and W. M. Clark, *J. Biol. Chem.*, **171**, (1947), 143.

56. A. H. Jackson and G. R. Dearden, *Ann. N.Y. Acad. Sci.*, **206**, (1973), 151.

57. E. B. Fleischer and M. Krishnamurthy, *J. Coord. Chem.*, **2**, (1972), 89.

58. H. Goff and L. O. Morgan, *Inorg. Chem.*, **15:9**, (1976), 2069.

59. K. R. Ashley, J. G. Leipoldt and V. K. Joshi, *Inorg. Chem.*, **19**, (1980), 1608.

60. D. Brault and M. Rougee, *Biochemistry*, **13:22**, (1974), 4591.

61. J. G. Leipoldt, S. S. Basson and D. R. Rabie, *J. inorg. nucl. Chem.*, **43:12**, (1981), 3239.

62. R. W. Ramette, *J. Chem. Educ.*, **44**, (1967), 647.

63. a. N. J. Rose and R. S. Drago, *J. Am. Chem. Soc.*, **81**, (1959), 6138.
b. R. M. Guidry and R. S. Drago, *J. Am. Chem. Soc.*, **95**, (1973), 6645.

64. F. J. C. Rossotti and H. Rossotti, The Determination of Stability Constants (McGraw-Hill, New York, 1961), p. 277.

65. P. George and G. I. H. Hanania, *Nature (London)*, **175**, (1955), 1034.

66. M. Krishnamurthy, *Inorganica Chimica Acta*, **25**, (1977), 215.

67. M. J. Payne and K. A. Berglund, *Mat. Res. Soc. Symp. Proc.*, **73**, (1986), 627.

68. K. Narayanaswamy, D. A. Russell and I. F Sevilla, *Talanta*, **35:2**, (1988), 83.

69. S. Luo and D. R. Walt, *Anal. Chem.*, **61**, (1989), 174.

70. L. M. Christian and W. R. Seitz, *Talanta*, **35:2**, (1988), 119.

71. N. Opitz and D. W. Lubbers, *Talanta*, **35:2**, (1988), 123.

72. T. P. Jones and M. D. Porter, *Anal. Chem.*, **60**, (1988), 404.

73. L. M. Ellerby, C. R. Nishida, F. Nishida, S. A. Yamanaka, B. Dunn, J. S. Valentine and J. I. Zink, *Science*, **255**, (28th Feb, 1992), 1113.

74. J. I. Dulebohn, B. V. Vlierberge, K. A. Berglund, R. B. Lessard, J. Yu and D. G. Nocera, *Mat. Res. Soc. Symp. Proc.*, **180**, (1990), 733.

75. C. K Chang, Department of Chemistry, Michigan State University.

76. U. S. Patent 2, 621,193, (assigned to E. I. Dupont De Nemours and Co., Inc.) June 27th, 1950.

77. R. T. Morrison and R. N. Boyd, Organic Chemistry, (Allyn &Bacon, Inc., Boston, 1987, 5th Edition), ch. 23.

78. C. D. Gagliardi and K. A. Berglund, *Mat. Res. Soc. Symp. Ser.*, **155**, (1989), 127.